NATIONAL ADVISORY COMMITTEE FOR AERONAUTICS

TECHNICAL NOTE 3022

METHOD FOR STUDYING HELICOPTER LONGITUDINAL MANEUVER STABILITY

By Kenneth B. Amer

Langley Aeronautical Laboratory
Langley Field, Va.

Washington
October 1953

CONTENTS

NATIONAL ADVISORY COMMITTEE FOR AERONAUTICS

TECHNICAL NOTE 3022

METHOD FOR STUDYING HELICOPTER LONGITUDINAL MANEUVER STABILITY

By Kenneth B. Amer

SUMMARY

Because of the importance of satisfactory maneuver stability for helicopter contact and instrument flying, a theoretical analysis of maneuver stability has been made. The results of the analysis are presented in the form of a chart which contains a boundary line separating combinations of significant longitudinal stability derivatives which result in satisfactory maneuver stability from combinations which result in unsatisfactory maneuver stability according to the criterion of NACA Technical Note 1983.

Good correlation is indicated for both a single-rotor helicopter and a tandem-rotor helicopter between maneuver stability as predicted by the chart and as measured during pull-up maneuvers. Thus, the theoretical analysis is indicated to be valid.

Techniques for measuring stability derivatives in flight are described. These derivatives are for use with the chart presented herein to aid in design studies of means for achieving at least marginal maneuver stability for a prototype helicopter or for a helicopter in the design stage that is similar to helicopters already flying.

In predicting the maneuver stability of a new type of helicopter, the stability derivatives for use with the chart presented herein must be theoretically predicted. The problem remains of predicting these derivatives with the desired accuracy where significant amounts of rotor stalling are present.

INTRODUCTION

The expanding uses of the helicopter in both military and civilian fields are emphasizing the need for satisfactory flying qualities under both contact and instrument conditions. In reference 1 is brought out the importance in forward flight under contact conditions of satisfactory maneuver stability, that is, no divergent tendency in pitch. In reference 2, blind-flying trials conducted in a single-rotor helicopter are

reported and it is concluded that "Changing the maneuver stability from unsatisfactory to satisfactory markedly reduced the effort required of the pilot to maintain a given flight path under instrument conditions. In addition, the danger due to divergent tendencies was removed." A criterion for maneuver stability is presented in reference 3, based on flying-qualities studies of single-rotor helicopters. The criterion is worded as follows:

> When the longitudinal control stick is suddenly displaced rearward 1 inch from trim (while in level flight at the maximum placard speed) and held fixed at this displacement, the time history of normal acceleration shall become concave downward within 2 seconds following the start of the maneuver.

It should be noted that the phrase "concave downward within 2 seconds" in this criterion refers to the slope of the normal-acceleration curve, that is, the slope shall reach its maximum value and begin to decrease within the given time interval. The significance of this criterion is that it calls for evidence within 2 seconds of the eventual peaking of the normal-acceleration time history. Subsequent studies on a tandem helicopter indicated this criterion to be generally applicable to tandem helicopters. This criterion is incorporated in the current requirements for military-helicopter flying qualities. This paper is presented in order to provide a basis for designers and the procurement agencies to use in studying the maneuver stability of a prospective helicopter.

The paper is divided into two parts. Part I is an analytical study of maneuver stability from which a chart is derived showing combinations of pertinent stability derivatives that result in a normal-acceleration time history that represents a case of marginal maneuver stability. Also in part I, the validity of the chart is checked against experimental data for both a single-rotor and a tandem-rotor helicopter.

In order to make use of the chart presented herein, the significant longitudinal-stability derivatives of the helicopter must either be theoretically predicted or measured. In part II of this paper, the difficulty of theoretically predicting the derivatives for this purpose is discussed and techniques for making flight measurements of stability derivatives are described. The mathematical manipulations needed to obtain the derivatives from flight data for use in the previous comparison are performed; thus, sample calculations are provided.

SYMBOLS

A_1, B_1 coefficients of $-\cos\psi$ and $-\sin\psi$, respectively, in expression for θ; therefore, lateral and longitudinal cyclic pitch, respectively, uncorrected for blade and control-system distortion, δ_3, or automatic control devices, radians

a_1 longitudinal tilt of rotor cone, radians

a' projection of angle between rotor force vector and axis of no feathering in plane containing flight path and axis of no feathering (for discussion of significance of axis of no feathering, see appendix of ref. 4)

a real part of conjugate complex roots of characteristic equation (denominator of eq. (23) set equal to zero)

b number of blades per rotor; also, imaginary part of conjugate complex roots of characteristic equation (denominator of eq. (23) set equal to zero)

C_T thrust coefficient, $\frac{T}{\pi R^2 \rho (\Omega R)^2}$

c blade-section chord, ft; also, b/i where b is imaginary part of complex root of characteristic equation

c_e equivalent blade chord (on thrust basis), $\frac{\int_0^R cr^2 dr}{\int_0^R r^2 dr}$, ft

d perpendicular distance between rotor shafts of a tandem helicopter, ft

e offset of center line of flapping hinge from center line of rotor shaft, ft

F force exerted by rotor blade on flapping hinge due to centrifugal acceleration, lb

g acceleration due to gravity, 32.2 ft/sec^2

h height of rotor hub(s) above center of gravity, ft

I_Y helicopter pitching moment of inertia about center of gravity, slug-ft^2

i incidence of plane perpendicular to rotor shaft, radians; also, $\sqrt{-1}$

L lift, positive upward, lb

M	pitching moment about center of gravity, positive nose-up, lb-ft
Δn	increment in normal acceleration from trim value, g units
q	helicopter pitching velocity, radians/sec
R	blade radius, ft
r	radial distance to blade element, ft
s	Laplace transform parameter
T	rotor thrust, lb
t	time
V	true airspeed of helicopter along flight path, fps
v	induced inflow velocity at rotor (always positive), fps
W	gross weight of helicopter, lb
α	rotor angle of attack; angle between flight path and plane perpendicular to axis of no feathering, positive when axis is inclined rearward, uncorrected for blade and control-system distortion, δ_3, or automatic control devices, radians
α_f	fuselage angle of attack, angle of attack of plane perpendicular to rotor shaft, radians
γ	angle of climb, radians
Δ,δ	increment
δ_3	angle in plane of rotation between perpendicular to blade-span axis and flapping-hinge axis, positive when an increase in flapping produces a decrease in blade pitch
Θ	instantaneous blade-section pitch angle; angle between line of zero lift of blade section and plane perpendicular to rotor shaft, uncorrected for blade and control-system distortion, δ_3, or automatic control devices, $\theta - A_1 \cos \psi - B_1 \sin \psi$, radians
θ	collective pitch, average value of Θ around azimuth, uncorrected for blade and control-system distortion, δ_3, or automatic control devices, radians

λ inflow ratio, $(V \sin \alpha - v)/\Omega R$

μ tip-speed ratio, $V \cos \alpha/\Omega R$ (assumed equal to $V/\Omega R$)

ρ mass density of air, slugs/cu ft

σ rotor solidity, $bc_e/\pi R$

ψ blade azimuth angle measured from downwind position in direction of rotation, radians

Ω rotor angular velocity, radians/sec

$\frac{\partial \Delta\theta}{\partial B_1}$ ratio of differential collective pitch to cyclic pitch due to longitudinal stick motion rigged into tandem helicopter

Stability derivatives:

Stability derivatives are indicated by subscript notation; for example, $\bar{L}_\alpha = \frac{\partial \bar{L}}{\partial \alpha}$. They are defined as follows:

$$\bar{L}_\alpha = L_{\bar{\theta}}\bar{\theta}_\alpha + L_\alpha$$

$$\bar{L}_q = L_q + L_{\bar{\theta}}\bar{\theta}_q - \bar{B}_{1_q}\left(L_{\bar{\theta}}\bar{\theta}_\alpha + L_\alpha\right)$$

$$\bar{M}_q = M_q + M_{\bar{\theta}}\left(\bar{\theta}_q - \bar{\theta}_\alpha \bar{B}_{1_q}\right) - \bar{B}_{1_q}\left(M_\alpha\right)_r + M_{\bar{B}_1}\bar{B}_{1_q}\left(1 - \bar{B}_{1_\alpha}\right)$$

$$\bar{M}_\alpha = \left(M_\alpha\right)_r + M_{\bar{\theta}}\bar{\theta}_\alpha + \bar{B}_{1_\alpha}M_{\bar{B}_1} + \left(M_\alpha\right)_{f+t}$$

$$K_1 = M_{\bar{B}_1} + \left(M_\alpha\right)_{f+t}$$

$$E = \frac{\bar{L}_q}{\bar{L}_\alpha}\left(\frac{K_1}{I_Y} - \frac{\bar{M}_\alpha}{I_Y}\right) = \frac{\bar{L}_q}{\bar{L}_\alpha I_Y}\left[M_{\bar{B}_1} - \left(M_\alpha\right)_r - M_{\bar{\theta}}\bar{\theta}_\alpha - B_{1_\alpha}M_{\bar{B}_1}\right]$$

Subscripts:

r rotor

f fuselage

t tail

c control motion during measurement of stability derivatives

p pilot's control motion in pull-up maneuver

0 trim or original value

1 modified flight condition at increased angle of attack

m measured

Superscripts:

$(\bar{\ })$ including effects of blade and control-system distortion, δ_3, and automatic control devices

$(\dot{\ })$ d/dt

I - ANALYTICAL PHASE OF MANEUVER-STABILITY STUDY

In this part of the report, the equations of motion applicable to the pull-up maneuver are derived and solved and the assumptions involved are discussed. Then the procedure involved in deriving the maneuver-stability chart is discussed and the chart is presented. From study of the chart, the stability derivatives that have a significant effect on maneuver stability are deduced. Finally, the validity of the chart is checked by a comparison, for both a single-rotor and a tandem-rotor helicopter, of maneuver stability as predicted by the chart and as measured during pull-up maneuvers. The stability derivatives for use in this comparison are obtained from flight data by techniques described in part II of this paper.

THEORETICAL ANALYSIS

In this section, the equations of motion applicable to the pull-up maneuver will be derived and solved.

Assumptions

Constant forward speed.- The assumption is made that the forward speed remains constant during the pull-up maneuver. This assumption, which is used in equivalent analyses for airplanes, is conservative if

the helicopter is stable with speed. The actual reduction in speed which occurs would produce a nose-down moment and a reduction in thrust. Both of these factors would tend to cause the normal-acceleration time history to become concave downward sooner. Thus, the assumption of no speed change is always conservative for helicopters with positive speed stability.

For other uses of the equations of motion, such as in studies of the long-period oscillation or in certain autopilot studies, it would be necessary to include the effects of variations in speed.

Small displacements, initial flight path level.- As in equivalent analyses for airplanes, the assumptions are made that the displacements from trim are small and the trim condition is in level flight.

Constant rotor speed.- Although the tendency exists for the rotor speed to increase during a pull-up, the assumption is made that the rotor speed is constant. A sample investigation of this assumption, which is discussed in the appendix, has indicated a resulting change of about 0.05 second in the time for the time history of normal acceleration to become concave downward. Also, future helicopters are likely to be equipped with governors to assist the pilot in preventing the rotor speed from exceeding the maximum allowable and to help limit maximum load factors. If a throttle-type governor is used, no corrections to the stability derivatives are necessary. If a pitch-type governor is used, corrections to the stability derivatives to account for the pitch change would be necessary. However, these corrections are felt to be beyond the scope of this paper.

Quasi-static conditions.- The assumption is made that the dynamic maneuver can be represented by a series of static conditions and hence the blade flapping coefficients and the rotor inflow and downwash velocities are always at their equilibrium values, determined by the instantaneous values of α, θ, μ, and q. Inasmuch as the order of magnitude of the time interval for the change in flight condition is 2 seconds, it is felt that the assumptions are justified except perhaps the flapping assumption for blades having a very low mass factor or very low flapping stability. For such blades, the need for considering the flapping as an additional degree of freedom would have to be investigated.

For other uses of the equations of motion, such as for autopilot studies, these quasi-static assumptions might not be valid at the higher end of the significant frequency range.

Lift due to elevator deflection neglected.- Where a helicopter is equipped with an elevator that moves with the longitudinal control, the change in lift due to elevator deflection is neglected.

Lift of fuselage and tail depend upon rotor angle of attack.- It will be assumed that the change in lift of the fuselage and tail is dependent upon changes in rotor angle of attack. A small error arises because the change in fuselage angle of attack differs from the change in rotor angle of attack by an amount equal to the change in longitudinal cyclic pitch. However, this error is insignificant inasmuch as the lift-curve slope of the fuselage and tail is considerably smaller than the lift-curve slope of the rotor.

Constant stability derivatives.- In order to solve the equations of motion by feasible methods, it is necessary to assume that the stability derivatives are constant during the pull-up maneuver. Failure to make this assumption would result in nonlinear differential equations, which are extremely tedious and difficult to solve. Actually, the derivative $\partial M/\partial \alpha$ does change during the maneuver because of nonlinearities as explained in reference 5. The derivative $\partial M/\partial \alpha$ as well as the other derivatives also varies during the maneuver if significant stalling occurs. Similarly, the derivatives also vary with the magnitude of the control deflection used to produce the maneuver. In order to handle these variations approximately, it might be assumed that the 1-inch stick deflection called for in the maneuver-stability criterion produces 1° of longitudinal cyclic pitch and results in a pull-up of 0.4g acceleration increment. Then, the stability derivatives can either be computed at 1.2g or by taking increments over the range from 1.0g to 1.4g. Also, they should be computed with the assumption that the 1° cyclic pitch change has already occurred.

Effects of blade and control-system distortion, δ_3, and automatic control devices accounted for by $\bar{B}_1$ and $\bar{\theta}$ derivatives.- It will be assumed that the effects of blade distortion, δ_3, and automatic control devices can be accounted for by derivatives of longitudinal cyclic pitch $\bar{B}_1$ and collective pitch $\bar{\theta}$ with respect to rotor angle of attack $\bar{\alpha}$ and pitching velocity q.

Equations of Motion

A system of axes based on the flight path is used. The equations of motion are derived on the basis of the previously discussed assumptions, one equation for equilibrium normal to the flight path, and one for equilibrium in pitch. Only changes in force and moment from trim values are considered.

Equilibrium normal to flight path.- The forces acting normal to the flight path during the pull-up maneuver are the changes in lift acting upward and the centrifugal inertia force due to the curved flight path acting downward. Thus,

$$L_q q + L_{\bar{\theta}} \Delta\bar{\theta} + L_{\bar{\alpha}} \Delta\bar{\alpha} - \frac{WV}{g} \dot{\gamma} = 0 \tag{1}$$

or

$$\dot{\gamma} - \frac{g}{WV} L_q q - \frac{g}{WV} L_{\bar{\theta}} \Delta\bar{\theta} - \frac{g}{WV} L_{\bar{\alpha}} \Delta\bar{\alpha} = 0 \tag{2}$$

From the definitions of $\Delta\alpha$ and $\Delta\bar{\alpha}$ and from the assumptions,

$$\Delta\bar{\alpha} = \Delta\alpha - \bar{B}_{1_{\bar{\alpha}}} \Delta\bar{\alpha} - \bar{B}_{1_q} q$$

where $\bar{B}_{1_{\bar{\alpha}}}$ and $\bar{B}_{1_q}$ are due to blade twist, δ_3, and automatic control devices.

Solving for $\Delta\bar{\alpha}$ and $\partial\Delta\bar{\alpha}/\partial\Delta\alpha$ yields

$$\Delta\bar{\alpha} = \frac{\Delta\alpha}{1 + \bar{B}_{1_{\bar{\alpha}}}} - \frac{\bar{B}_{1_q} q}{1 + \bar{B}_{1_{\bar{\alpha}}}} \tag{3}$$

and

$$\frac{\partial\Delta\bar{\alpha}}{\partial\Delta\alpha} = \frac{1}{1 + \bar{B}_{1_{\bar{\alpha}}}} \tag{4}$$

Also, with the assumption of no change in pilot's pitch-lever position

$$\Delta\bar{\theta} = \bar{\theta}_{\bar{\alpha}} \Delta\bar{\alpha} + \bar{\theta}_q q \tag{5}$$

where $\bar{\theta}_{\bar{\alpha}}$ and $\bar{\theta}_q$ are also due to blade twist, δ_3, and automatic control devices. Substituting equation (3) into equation (5) yields

$$\Delta\bar{\theta} = \frac{\bar{\theta}_{\bar{\alpha}}\,\Delta\alpha}{1 + \bar{B}_{1_{\bar{\alpha}}}} + \left(\bar{\theta}_q - \frac{\bar{\theta}_{\bar{\alpha}}\bar{B}_{1_q}}{1 + \bar{B}_{1_{\bar{\alpha}}}}\right)q \tag{6}$$

Substituting equations (3), (4), and (6) into equation (2) gives

$$\dot{\gamma} - \frac{g}{WV}\bar{L}_\alpha\,\Delta\alpha - \frac{g}{WV}\bar{L}_q q = 0 \tag{7}$$

where

$$\bar{L}_\alpha = \frac{L_{\bar{\theta}}\bar{\theta}_{\bar{\alpha}} + L_{\bar{\alpha}}}{1 + \bar{B}_{1_{\bar{\alpha}}}} = L_{\bar{\theta}}\bar{\theta}_\alpha + L_\alpha \tag{8}$$

and

$$\bar{L}_q = L_q + L_{\bar{\theta}}\bar{\theta}_q + \frac{-L_{\bar{\theta}}\bar{\theta}_{\bar{\alpha}}\bar{B}_{1_q} - L_{\bar{\alpha}}\bar{B}_{1_q}}{1 + \bar{B}_{1_{\bar{\alpha}}}} = L_q + L_{\bar{\theta}}\bar{\theta}_q - \bar{B}_{1_q}\left(L_{\bar{\theta}}\bar{\theta}_\alpha + L_\alpha\right) \tag{9}$$

The first form of the expressions for $\bar{L}_\alpha$ and $\bar{L}_q$ is appropriate for computing purposes, while the second form is appropriate for full-scale measuring purposes.

Equilibrium in pitch.- There are five pitching moments acting during the maneuver. These are moments due to collective-pitch change, damping in pitch, angle-of-attack stability of rotor and fuselage-tail combination, control displacement, and inertia.

Thus,

$$M_{\bar{\theta}}\,\Delta\bar{\theta} + M_q q + \left(M_{\bar{\alpha}}\right)_r\,\Delta\bar{\alpha} + \left(M_\alpha\right)_{f+t}\,\Delta\alpha_f + M_{\bar{B}_1}\,\Delta\bar{B}_1 - I_Y\dot{q} = 0 \tag{10}$$

The terms $M_{\bar{\theta}}\,\Delta\bar{\theta}$, $M_q q$, and $\left(M_{\bar{\alpha}}\right)_r\,\Delta\bar{\alpha}$ account for the pitching moments due to thrust-vector and tip-path-plane tilts with respect to

the axis of no feathering. The term $M_{\bar{B}_1}\Delta\bar{B}_1$ accounts for pitching moments due to a tilt of the axis of no feathering with respect to the rotor shaft. Inasmuch as

$$\Delta\alpha_f = \Delta\bar{\alpha} + \Delta\bar{B}_1 \tag{11}$$

equation (10) can be written as follows:

$$\dot{q} - \frac{M_{\bar{\theta}}}{I_Y}\Delta\bar{\theta} - \frac{M_q}{I_Y}q - \frac{\left(M_{\bar{\alpha}}\right)_r + \left(M_\alpha\right)_{f+t}}{I_Y}\Delta\bar{\alpha} = \frac{M_{\bar{B}_1} + \left(M_\alpha\right)_{f+t}}{I_Y}\Delta\bar{B}_1 \tag{12}$$

Also, by assumption,

$$\Delta\bar{B}_1 = \Delta B_{1_p} + \bar{B}_{1_{\bar{\alpha}}}\Delta\bar{\alpha} + \bar{B}_{1_q}q \tag{13}$$

No bar is placed above the ΔB_{1_p} term because changes in B_{1_p} due to twist, and so forth, are included in the $\bar{B}_{1_{\bar{\alpha}}}$ term. Combining equations (3) and (13) yields

$$\Delta\bar{B}_1 = \Delta B_{1_p} + \frac{\bar{B}_{1_\alpha}\Delta\alpha}{1 + \bar{B}_{1_{\bar{\alpha}}}} - \frac{\bar{B}_{1_{\bar{\alpha}}}B_{1_q}q}{1 + \bar{B}_{1_{\bar{\alpha}}}} + \bar{B}_{1_q}q \tag{14}$$

Substituting equations (3), (4), (6), and (14) into equation (12) gives

$$\dot{q} - \frac{\bar{M}_q}{I_Y}q - \frac{\bar{M}_\alpha}{I_Y}\Delta\alpha = \frac{K_1}{I_Y}\Delta B_{1_p} \tag{15}$$

where

$$\bar{M}_q = M_q + M_{\bar{\theta}}\left(\bar{\theta}_q - \frac{\bar{\theta}_{\bar{\alpha}}\bar{B}_{1_q}}{1 + \bar{B}_{1_{\bar{\alpha}}}}\right) - \frac{\left(M_{\bar{\alpha}}\right)_r B_{1_q}}{1 + \bar{B}_{1_{\bar{\alpha}}}} + M_{\bar{B}_1}\bar{B}_{1_q}\left(1 - \frac{\bar{B}_{1_{\bar{\alpha}}}}{1 + \bar{B}_{1_{\bar{\alpha}}}}\right)$$

$$= M_q + M_{\bar{\theta}}\left(\bar{\theta}_q - \bar{\theta}_\alpha\bar{B}_{1_q}\right) - \bar{B}_{1_q}\left(M_\alpha\right)_r + M_{\bar{B}_1}\bar{B}_{1_q}\left(1 - \bar{B}_{1_\alpha}\right) \tag{16}$$

$$\bar{M}_\alpha = \frac{\left(M_{\bar{\alpha}}\right)_r + M_{\bar{\theta}}\bar{\theta}_{\bar{\alpha}} + \bar{B}_{1_{\bar{\alpha}}}M_{\bar{B}_1}}{1 + \bar{B}_{1_{\bar{\alpha}}}} + \left(M_\alpha\right)_{f+t}$$

$$= \left(M_\alpha\right)_r + M_{\bar{\theta}}\bar{\theta}_\alpha + \bar{B}_{1_\alpha}M_{\bar{B}_1} + \left(M_\alpha\right)_{f+t} \tag{17}$$

$$K_1 = M_{\bar{B}_1} + \left(M_\alpha\right)_{f+t} \tag{18}$$

As for $\bar{L}_\alpha$ and $\bar{L}_q$, the first form of the expressions for $\bar{M}_q$ and $\bar{M}_\alpha$ is appropriate for computing purposes, while the second form is appropriate for measuring purposes.

Equation relating $\Delta\alpha$, γ, and q.- Inasmuch as the two equations of motion, equations (7) and (15), contain three variables, a third equation must be developed before a solution can be obtained. From examination of figure 1 it can be seen that, for the pull-up maneuver,

$$\alpha = i - \gamma - B_{1_p}$$

therefore

$$\Delta\alpha = \Delta i - \Delta\gamma - \Delta B_{1_p}$$

or

$$\Delta\alpha = \int_0^t q\,dt - \gamma - \Delta B_{l_p} \tag{19}$$

Solution of Equations of Motion

Procedure.- Equations (7), (15), and (19) constitute three simultaneous equations with three dependent variables α, q, and γ and an input variable ΔB_{l_p}. They are solved here by means of the Laplace transformation for γ as a function of time for a step input of B_{l_p}, simulating a pull-up maneuver. Inasmuch as

$$\Delta n = \frac{V}{g}\frac{\partial \gamma}{\partial t} \tag{20}$$

then

$$\frac{\partial \Delta n}{\partial t} = \frac{V}{g}\frac{\partial^2 \gamma}{\partial t^2} \tag{21}$$

Thus, the solution for γ will be differentiated twice and multiplied by V/g to get $\partial\Delta n/\partial t$ inasmuch as the point at which the normal-acceleration time history becomes concave downward corresponds to a point of maximum slope $\partial\Delta n/\partial t$. Then combinations of the stability derivatives which give maximum $\partial\Delta n/\partial t$ at $t = 2$ seconds will be determined by iteration. The alternative procedure was considered of differentiating the solution once more to get $\partial^2\Delta n/\partial t^2$ and determining the combination of stability derivatives to give $\partial^2\Delta n/\partial t^2 = 0$ at $t = 2$ seconds. However, the alternative procedure did not appear to be superior to the first procedure discussed.

Laplace transformation of equations.- Taking the Laplace transform of equations (7), (15), and (19) by means of the table of transforms in reference 6 results in the following set of equations:

$$\left.\begin{aligned} s\gamma(s) - \frac{g}{WV}\bar{L}_q q(s) \quad & - \frac{g}{WV}\bar{L}_\alpha \Delta\alpha(s) = 0 \\ \left(s - \frac{\bar{M}_q}{I_Y}\right)q(s) - \frac{\bar{M}_\alpha}{I_Y}\Delta\alpha(s) \quad & = \frac{K_1}{I_Y}\frac{\Delta B_{1_p}}{s} \\ \gamma(s) - \frac{q(s)}{s} \quad + \Delta\alpha(s) \quad & = -\frac{\Delta B_{1_p}}{s} \end{aligned}\right\} \tag{22}$$

Equations (22) constitute a set of simultaneous algebraic equations which can be solved for $\gamma(s)$ by means of determinants. Thus,

$$\gamma(s) = \frac{\begin{vmatrix} 0 & -\frac{g}{WV}\bar{L}_q & -\frac{g}{WV}\bar{L}_\alpha \\ \frac{K_1}{I_Y}\frac{\Delta B_{1_p}}{s} & s - \frac{\bar{M}_q}{I_Y} & -\frac{\bar{M}_\alpha}{I_Y} \\ -\frac{\Delta B_{1_p}}{s} & -\frac{1}{s} & 1 \end{vmatrix}}{\begin{vmatrix} s & -\frac{g}{WV}\bar{L}_q & -\frac{g}{WV}\bar{L}_\alpha \\ 0 & s - \frac{\bar{M}_q}{I_Y} & -\frac{\bar{M}_\alpha}{I_Y} \\ 1 & -\frac{1}{s} & 1 \end{vmatrix}} \tag{23}$$

Solution for $\partial\Delta n/\partial t$.- The expression for $\gamma(s)$ was expanded and split up by partial fractions. Then the inverse transform was taken to get $\gamma(t)$ by using once again the table of transforms of reference 6. Then, with the use of equation (21), the following expression was obtained:

$$\frac{\partial \Delta n/\partial t}{-\Delta B_{l_p} \bar{L}_\alpha / W} = e^{at} \left\{ -\left(\frac{g}{WV}\bar{L}_\alpha + E\right)\cos bt + \left[-\frac{K_1}{b\bar{I}_Y} - b + \frac{a}{b}\left(a - \frac{\bar{M}_q}{\bar{I}_Y} - E\right)\right]\sin bt \right\} \tag{24}$$

where

$$E = \frac{\bar{L}_q}{\bar{L}_\alpha}\left(\frac{K_1}{\bar{I}_Y} - \frac{\bar{M}_\alpha}{\bar{I}_Y}\right) = \frac{\bar{L}_q}{\bar{L}_\alpha \bar{I}_Y}\left(M_{\bar{B}_1} - M_{\alpha_r} - M_{\bar{\theta}}\bar{\theta}_\alpha - B_{l_\alpha} M_{\bar{B}_1}\right) \tag{25}$$

or (considering the usual magnitude of the terms)

$$E \approx \frac{\bar{L}_q}{\bar{L}_\alpha}\frac{M_{\bar{B}_1}}{\bar{I}_Y}$$

and $a \pm bi$ are the roots of the equation formed by setting the denominator of equation (23) equal to zero (characteristic equation) and can be put into the following form:

$$a = \frac{\frac{\bar{M}_q}{\bar{I}_Y} + E - \left(\frac{g}{WV}\bar{L}_\alpha + E\right)}{2} \tag{26}$$

and

$$b = \sqrt{-\frac{\bar{M}_\alpha}{\bar{I}_Y}\left(1 - \frac{g}{WV}\bar{L}_q\right) + \frac{\bar{M}_q}{\bar{I}_Y}E + \left(\frac{g}{WV}\bar{L}_\alpha + E\right)E - \left(\frac{\bar{M}_q}{\bar{I}_Y} + E\right)\left(\frac{g}{WV}\bar{L}_\alpha + E\right) - a^2} \tag{27}$$

If b is imaginary (characteristic equation has real roots), equation (24) can be put into more convenient form by letting $b = ic$. Then, by use of the relations between trigonometric and hyperbolic functions,

$$\frac{\partial \Delta n / \partial t}{-\Delta B_{l_p} \bar{l}_\alpha / W} = e^{at} \left\{ - \left(\frac{g}{WV} \bar{l}_\alpha + E \right) \cosh ct + \left[- \frac{K_1}{c I_Y} + c + \frac{a}{c} \left(a - \frac{\bar{M}_q}{I_Y} - E \right) \right] \sinh ct \right\} \tag{28}$$

MANEUVER-STABILITY CHART

In this section a chart will be derived which indicates the combinations of stability derivatives which produce marginal maneuver stability.

Significant Stability Derivatives

Examination of equations (24) to (28) indicates the following parameters to affect the time for the normal-acceleration time history to become concave downward:

$$\frac{\bar{M}_q}{I_Y} + E$$

$$\frac{\bar{M}_\alpha}{I_Y} \left(1 - \frac{g}{WV} \bar{l}_q \right) - \frac{\bar{M}_q}{I_Y} E - \left(\frac{g}{WV} \bar{l}_\alpha + E \right) E$$

$$\frac{g}{WV} \bar{l}_\alpha + E$$

$$\frac{K_1}{I_Y}$$

Calculations indicate the parameter K_1/I_Y, which depends primarily on control power, to be of only minor importance. The significance of the three remaining parameters can be better appreciated by simplifying to the case of $\bar{L}_q = 0$. The three parameters then become $\frac{\bar{M}_q}{I_Y}$, $\frac{\bar{M}_\alpha}{I_Y}$, and $\frac{g}{WV}\bar{L}_\alpha$. Thus, maneuver stability is indicated to be a function of damping in pitch and angle-of-attack stability as discussed in reference 1, of the moment of inertia in pitch, of the lift-curve slope, and of the lift due to pitching of the helicopter.

Calculation Procedure

The procedure for calculating the desired combinations of stability derivatives is based on the reasonable assumption that if $\Delta\dot{n}$ is maximum at $t = 2$ seconds (Δn curve concave downward at 2 seconds), then $\Delta\dot{n}$ at $t = 1.95$ seconds is equal to $\Delta\dot{n}$ at $t = 2.05$ seconds. Values of b, K_1/I_Y, and $\frac{g}{WV}\bar{L}_\alpha + E$ were assumed and values of $\frac{\Delta\dot{n}}{-\Delta B_{1_p}\bar{L}_\alpha/W}$ at $t = 1.95$ seconds and $t = 2.05$ seconds were calculated for two arbitrary values of $\frac{\bar{M}_q}{I_Y} + E$ from equation (26) and then equation (24) or (28).

A first approximation to the correct value of $\frac{\bar{M}_q}{I_Y} + E$ was obtained by interpolation or extrapolation of the percentage difference

$$\frac{\Delta\dot{n}_{t=2.05} - \Delta\dot{n}_{t=1.95}}{\Delta\dot{n}_{t=1.95}} \tag{29}$$

corresponding to each of the two values of $\frac{\bar{M}_q}{I_Y} + E$. This first approximation of $\frac{\bar{M}_q}{I_Y} + E$ was inserted back into equation (26) and then (24) or (28) and the interpolation procedure was repeated. This iteration process was continued until the quantity given by expression (29) was less than 0.01, so that the percentage difference in slopes at $t = 2.05$

and $t = 1.95$ was less than 1 percent. Then, the corresponding value of the parameter

$$\frac{\bar{M}_\alpha}{I_Y}\left(1 - \frac{g}{WV}\bar{L}_q\right) - \frac{\bar{M}_q}{I_Y}E - \left(\frac{g}{WV}\bar{L}_\alpha + E\right)E$$

was obtained from equation (27).

As mentioned previously, the parameter K_1/I_Y, which depends primarily upon control power, was indicated to be of only minor importance. Thus, for simplicity, it was decided that only the most unfavorable value of K_1/I_Y would be used. Sample calculations indicated a reduction in K_1/I_Y to be mildly unfavorable. Thus, a value approximately one-half that of a typical present-day helicopter was used throughout the calculations.

Form of Chart

In figure 2 are presented plots of the parameter

$$\frac{\bar{M}_\alpha}{I_Y}\left(1 - \frac{g}{WV}\bar{L}_q\right) - \left(\frac{g}{WV}\bar{L}_\alpha + E\right)E - \frac{\bar{M}_q}{I_Y}E$$

against the parameter $\frac{\bar{M}_q}{I_Y} + E$ for various values of the parameter $\frac{g}{WV}\bar{L}_\alpha + E$ obtained from the previously described procedure. As discussed in reference 1, increases in angle-of-attack stability or in damping in pitch (more negative $\bar{M}_\alpha$ or $\bar{M}_q$) improve maneuver stability. Thus, for each value of $\frac{g}{WV}\bar{L}_\alpha + E$, the region below and to the left of the curve is satisfactory.

Figure 2 indicates an increase in $\bar{L}_\alpha$, which is the lift-curve slope, to be stabilizing in that an increasing satisfactory region exists for increasing values of the parameter. In addition, figure 2 shows an increase in pitching moment of inertia I_Y to be destabilizing.

Figure 2 is not in a very convenient form because of the overlapping regions of satisfactory and unsatisfactory maneuver stability for the different values of the lift-curve-slope parameter.

It was noted that, for a given value of the damping-in-pitch parameter, the value of the angle-of-attack stability parameter was approximately proportional to the lift-curve-slope parameter. Hence, it was found, by trial and error, that if the angle-of-attack stability parameter of figure 2 were modified to the parameter

$$\frac{\frac{\bar{M}_\alpha}{I_Y}\left(1 - \frac{g}{WV}\bar{L}_q\right) - \left(\frac{g}{WV}\bar{L}_\alpha + E\right)E - \frac{\bar{M}_q}{I_Y}E + 0.70 + 0.58\left(\frac{\bar{M}_q}{I_Y} + E\right) + 0.12\left(\frac{\bar{M}_q}{I_Y} + E\right)^2}{\frac{g}{WV}\bar{L}_\alpha + E}$$

a single boundary curve would be produced.

In figure 3 is presented an alternate form of chart using this modified angle-of-attack stability parameter. The single curve of figure 3 represents approximately the entire range of lift-curve slope covered in figure 2. Thus, figure 3, although somewhat less accurate than figure 2, is considered to be a more convenient form of chart to use.

COMPARISON OF MANEUVER STABILITY AS MEASURED IN FLIGHT WITH PREDICTIONS OF CHART OF THIS PAPER

In order to check the validity of the procedure used to obtain the chart presented herein, comparison is made of maneuver stability as measured in flight with predictions of the chart of this paper. The stability derivatives for use with the chart are determined in part II of this paper. The comparison is made for the single-rotor helicopter of figure 4 with and without a horizontal tail surface, and for the tandem-rotor helicopter of figure 5 in two different flight conditions. The horizontal tail used on the single-rotor helicopter is shown in figure 6 and its principal dimensions are given in figure 7.

In figure 8 are presented time histories of control position and normal acceleration during pull-up maneuvers at approximately 70 knots indicated airspeed. Figures 8(a) and 8(b) are for the single-rotor helicopter of figure 4 in level flight with tail surface off and on at 0° incidence with respect to the rotor shaft, respectively. Figures 8(c) and 8(d) are for the tandem-rotor helicopter of figure 5 in level flight

and partial-power descent, respectively, with the center of gravity 13 inches forward of the midpoint between the rotor shafts.

The data from which the normal-acceleration time histories of figures 8(a) and 8(b) were obtained were similar to those shown in figures 8(c) and 8(d). The normal accelerometer reflects the vibration of the helicopter which necessitates fairing the data as indicated in figures 8(c) and 8(d). The result is some inaccuracy in determining the time for the normal-acceleration time history to become concave downward but the error is considered insignificant.

In figure 9, the theoretical curve of figure 3 is replotted along with six data points, four of them corresponding to the four helicopter configurations for which pull-up time histories are presented in figure 8 and for which stability derivatives are computed in part II of this paper. Adjacent to each of these four points is given the approximate time for the corresponding normal-acceleration time history of figure 8 to become concave downward. The time history of normal acceleration of figure 8(a) is divergent throughout and the corresponding data point in figure 9 is labeled accordingly.

Two additional data points are plotted in figure 9. One data point is for the single-rotor helicopter with tail on, but with a tail-incidence setting of 7° nose up. It was assumed that this change in tail setting did not change $\bar{I}_\alpha$ or $\bar{M}_q$ from the value for the configuration with 0° tail incidence. The effect on $\bar{M}_\alpha$ due to the change in down load on the tail surface was estimated theoretically. The second additional data point is for the tandem helicopter in level flight but with approximately 5 percent higher thrust coefficient than for the previous level-flight condition and with the center of gravity approximately at the midpoint between the rotors. The effect of the center-of-gravity change on the value of $\bar{M}_\alpha$ for the previous level-flight condition was computed theoretically, changes in $\bar{M}_\alpha$ due to changes in rear-rotor stalling being neglected. The slight effect of the 5-percent increase in thrust coefficient on $\bar{I}_\alpha$ and $\bar{M}_q$ was also computed theoretically, effects of changes in rear-rotor stalling being neglected. The times for the corresponding normal-acceleration time histories to become concave downward were obtained from time histories similar to those in figure 8 and are given adjacent to each point.

The theoretical curve of figure 9 (and hence of fig. 3) is indicated to be qualitatively correct for both single- and tandem-rotor helicopters in separating configurations which have satisfactory maneuver stability according to the criterion of reference 3 from those which have unsatisfactory maneuver stability. This can be seen by noting that the points for which the normal-acceleration time history becomes concave downward in less than 2 seconds fall in the satisfactory region while those for

times to become concave downward of more than 2 seconds fall in the unsatisfactory region. Thus, the analytical procedure used to obtain the chart of figure 9 (and fig. 3) is indicated to be valid.

II - FLIGHT MEASUREMENT OF LONGITUDINAL-STABILITY DERIVATIVES

In order to make use of the chart presented herein for evaluating the maneuver stability of a prospective helicopter, the significant longitudinal-stability derivatives of the helicopter must either be theoretically predicted or measured. For a new type of helicopter in the design stage, it would be necessary to compute the longitudinal-stability derivatives of the design. If no stalling is present, the derivatives of the rotor can be predicted on the basis of the available rotor theory of references 7 to 9. However, it is usually necessary to take account of rotor stalling because, as pointed out in several previous NACA papers (see, for example, ref. 10), the optimum flight condition from the standpoint of performance is approximately that at which stalling just begins. A helicopter designed to fly near this optimum condition in cruising flight would always encounter rotor stalling during a pull-up at cruising speed or higher.

Preliminary studies indicate large effects of rotor stalling on longitudinal-stability derivatives. Thus, in evaluating the maneuver stability of a new type of helicopter in the design stage, these stalling effects must be known, at least approximately, before the rotor longitudinal-stability derivatives can be computed and use made of the chart presented herein. More detailed discussion of the effects of stalling on rotor longitudinal-stability derivatives is beyond the scope of this paper.

For a prototype helicopter that is in the flight-test stage, or for a helicopter in the design stage that is similar to a helicopter already flying, the necessary stability derivatives can be measured in flight by the techniques described in this part of the paper. These measured stability derivatives can be used with the chart presented herein in studying the maneuver stability of these helicopters. For example, if tests such as that called for in the criterion of reference 3 indicate a prototype helicopter to have maneuver instability, the significant longitudinal-stability derivatives of the helicopter can be measured in flight by means of the techniques described in this section and then plotted on the chart. Then, the magnitude of the changes in the stability derivatives necessary to produce marginal maneuver stability can be determined. These theoretically predicted changes can be used as bases for design studies of practical methods of achieving satisfactory maneuver stability. The most practical changes to make are probably in $\bar{M}_\alpha$ and $\bar{M}_q$ by means such as those discussed in reference 1. It should be noted that changes in $\bar{M}_q$ vary the modified angle-of-attack stability parameter.

After the techniques for flight measurement of the significant derivatives are described, sample calculations are performed. The calculations, which are for the helicopters in figures 4 and 5, are used in the comparison discussed in the previous section.

TECHNIQUE OF FLIGHT MEASUREMENT OF SIGNIFICANT LONGITUDINAL-STABILITY DERIVATIVES

In this section, techniques for measuring in flight the derivatives of lift and pitching moment with respect to angle of attack and pitching velocity are discussed.

Lift-Curve-Slope and Angle-of-Attack Stability Derivatives

The technique used to measure the lift-curve-slope and angle-of-attack stability derivatives of a helicopter in flight can best be understood by comparison with a possible wind-tunnel technique.

Wind-tunnel technique.- Assume a helicopter mounted in a wind tunnel at a particular flight condition, with pitching moments about the center of gravity trimmed to zero by means of longitudinal positioning of the control stick. Let this original flight condition be specified by the three parameters μ_0, θ_0, and $\left(C_T/\sigma\right)_0$.

As indicated in reference 9, the flight condition of a rotor is specified by three independent parameters. In reference 9, the three parameters are μ, θ, and λ, where λ is the inflow ratio. For convenience in this discussion, the parameter C_T/σ is used instead of λ. The value of the rotor angle of attack is fixed by the values of μ, C_T/σ, and θ.

Next, assume that the angle of attack of the helicopter is increased, so that an increase in thrust is produced, the rotor speed and pitch lever being kept constant; also, assume that the control stick is moved longitudinally to retrim the pitching moments to zero. The modified flight condition is specified by the following parameters:

$$\mu_1,\ \theta_1,\ \left(C_T/\sigma\right)_1$$

where

$$\mu_1 = \mu_0$$

$$\theta_1 = \theta_0$$

$$\left(C_T/\sigma\right)_1 > \left(C_T/\sigma\right)_0$$

The lift-curve slope of the helicopter, whether single or tandem rotor, can be determined from the measured changes in thrust and angle of attack of the axis of no feathering.

The angle-of-attack stability can be computed from the measured change in control-stick position. If the control stick were returned to its initial position, a pitching moment would be produced on a single-rotor helicopter equal to

$$\Delta M = \Delta B_{1_c}\left(T_0 + \Delta T\right)h\left(1 + \frac{\partial a'}{\partial \alpha}\right) + \Delta B_{1_c}\frac{bFe}{2}\left(1 + \frac{\partial a_1}{\partial \alpha}\right)$$

or

$$\Delta M = \Delta B_{1_c}T_0\left[1 + \frac{\Delta\left(C_T/\sigma\right)}{\left(C_T/\sigma\right)_0}\right]h\left(1 + \frac{\partial a'}{\partial \alpha}\right) + \Delta B_{1_c}\frac{bFe}{2}\left(1 + \frac{\partial a_1}{\partial \alpha}\right) \qquad (30)$$

where ΔB_{1_c} is the measured change in cyclic pitch.

The first term in equation (30) accounts for pitching moments due to thrust-vector tilt; the second term accounts for those due to the centrifugal forces in the blades combined with the offset flapping hinges. The second term was derived by assuming that the centrifugal forces in the blades act along the blade spanwise axis. The $\partial a'/\partial \alpha$ and $\partial a_1/\partial \alpha$ terms account for the usual instability of the rotor with angle of attack. Inasmuch as these terms are normally much less than unity, they can be obtained to a sufficient degree of accuracy, by neglecting any effects of stalling, from references 7 and 9. If a horizontal tail surface is linked to the control stick, its contribution to ΔM must be added to equation (30). The angle-of-attack stability is obtained by dividing ΔM by $\Delta \alpha$.

For a tandem helicopter, the pitching moment due to returning the stick to its original position is

$$\Delta M = 2\,\Delta M_{\text{single rotor}} + \Delta T\,\frac{d}{2}$$

$$= 2\,\Delta M_{\text{single rotor}} + \Delta B_{1_c}\,\frac{\partial \Delta\theta}{\partial B_1}\,\frac{\partial\left(C_T/\sigma\right)}{\partial\theta}\,\frac{T_0}{\left(C_T/\sigma\right)_0}\,\frac{d}{2} \qquad (31)$$

where

ΔT difference in thrust between the two rotors

T_0 original thrust per rotor

$\frac{\partial \Delta\theta}{\partial B_1}$ ratio of differential collective pitch to cyclic pitch due to longitudinal stick motion rigged into the tandem helicopter

and where $\Delta M_{\text{single rotor}}$ is given by equation (30) and $\frac{\partial\left(C_T/\sigma\right)}{\partial\theta}$ can be obtained from the charts of reference 7. Alternatively, $\frac{\partial\left(C_T/\sigma\right)}{\partial\theta}$ could be obtained by measuring the change in thrust with change in collective pitch.

The angle-of-attack stability is again obtained by dividing ΔM by $\Delta\alpha$.

Flight technique.- If it were attempted to use the wind-tunnel technique in flight, a complication would develop in that, as soon as the angle of attack was increased, the resulting thrust increase would produce a pull-up, and hence unsteady flight conditions. The basic feature of the flight technique described herein is to obtain the increase in C_T/σ by reducing the rotor speed and retaining the original value of thrust, so that data can be taken under steady flight conditions. The pitch lever is kept fixed as in the wind-tunnel technique. The forward speed is reduced in proportion to the rotor speed to maintain the same tip-speed ratio.

In more detail, the flight technique consists of taking approximately a 2-minute record of the original flight condition. The forward speed and rotor speed are then reduced in proportion, the latter by reducing power. Because of the transient reduction in thrust, the helicopter will start to descend; the descent will result in an increase in rotor angle of attack sufficient to bring the thrust back to the original value, and hence equal to the weight. Another 2-minute record is taken. Inasmuch as both flight conditions are steady, the longitudinal stick position must be such as to trim pitching moments to zero.

Thus, if the techniques are considered in terms of nondimensional quantities, the flight technique is identical to the wind-tunnel technique. The original values of μ, C_T/σ, and θ are duplicated as are the modified values of μ, C_T/σ, and θ. The change in angle of attack in flight is the same as in the wind tunnel inasmuch as α is specified when μ, C_T/σ, and θ are specified.

The lift-curve-slope derivative, whether for a single or a tandem helicopter, can once again be determined from $\frac{\Delta(C_T/\sigma)}{\Delta\alpha}$. The change in C_T/σ can be obtained by measuring the rotor speed during the two runs. The change in α can be obtained by measuring forward speed, rate of descent, longitudinal fuselage inclination, and longitudinal cyclic pitch during the two runs.

The angle-of-attack stability at the normal value of rotor speed can be obtained as in the wind tunnel by using equations (30) or (31) and the measured change in longitudinal stick position. The derivative $\frac{\partial(C_T/\sigma)}{\partial\theta}$ for equation (31) can be measured in flight, if desired, by performing collective-pitch pull-ups.

Methods for measuring in flight many of the quantities mentioned in this section are discussed in reference 11.

Additional considerations in the use of the flight technique.- In the section entitled "Assumptions," it is suggested that, because the stability derivatives may not be constant, a pull-up of 1.4g be assumed and the derivatives be evaluated at 1.2g or over the range from 1.0g to 1.4g. Thus, for the determination in flight of the lift-curve-slope and angle-of-attack stability derivatives, the percentage reduction in rotor speed in going from the original condition to the modified condition should be about one-half the percentage increase in normal acceleration. For the test helicopters of figures 4 and 5, a reduction in rotor speed of no more than approximately 10 percent is permitted. Although the derivatives thus measured correspond to a 1.2g pull-up, the actual pull-ups made were somewhat larger. For this reason, the measured lift-curve-slope and angle-of-attack stability derivatives may be somewhat in error. This error

would be more serious if large amounts of stalling, and hence nonlinearity in the stability derivatives, were present.

One term that must be added to the angle-of-attack stability as measured in flight for use in the pull-up analysis is the contribution due to the displacement of the stick from its trim position, as mentioned in the section on "Assumptions." This term arises from the resulting displacement of the thrust vector from its trim position so that increases in rotor thrust have a different moment arm about the center of gravity. This correction is to the $\left(M_\alpha\right)_r$ term in $\bar{M}_\alpha$. Thus,

$$\delta\left(M_\alpha\right)_r = -\Delta B_{1_p}\left(1 + \frac{\partial a'}{\partial \alpha}\right)\frac{\Delta T}{\Delta \alpha}\, h$$

$$= -\Delta B_{1_p}\left(1 + \frac{\partial a'}{\partial \alpha}\right) h\, \frac{\Delta\left(C_T/\sigma\right)}{\Delta \alpha}\, \frac{T_O}{\left(C_T/\sigma\right)_O} \tag{32}$$

As also mentioned in the section on "Assumptions," ΔB_{1_p} might normally be assumed equal to 1°. However, inasmuch as ΔB_{1_p} was measured during the test pull-ups to be discussed, the measured value will be used.

For the special case of the single-rotor helicopter with zero offset of the flapping hinges, the correction term of equation (32) can be put in more convenient form as a correction to the ΔB_1 used in equation (30) as follows:

$$\Delta M = \delta\, \Delta B_{1_c} T_O \left[1 + \frac{\Delta\left(C_T/\sigma\right)}{\left(C_T/\sigma\right)_O}\right] h\left(1 + \frac{\partial a'}{\partial \alpha}\right)$$

$$= -\Delta B_{1_p}\left(1 + \frac{\partial a'}{\partial \alpha}\right) h\, \Delta\left(\frac{C_T}{\sigma}\right)\frac{T_O}{\left(C_T/\sigma\right)_O}$$

Solving for $\delta \Delta B_{1_c}$ yields

$$\delta \Delta B_{1_c} = -\Delta B_{1_p} \frac{\frac{\Delta(C_T/\sigma)}{(C_T/\sigma)_0}}{1 + \frac{\Delta(C_T/\sigma)}{(C_T/\sigma)_0}} \tag{33}$$

The quantity $\Delta(C_T/\sigma)$ in equation (33) is the increase in C_T/σ achieved during the flight measurement of angle-of-attack stability, inasmuch as $\delta \Delta B_{1_c}$ is used as a correction term to ΔB_{1_c} in equation (30).

Another error in the flight technique of measuring the lift-curve-slope and angle-of-attack stability derivatives arises if the rotor blades undergo a significant amount of twist. Inasmuch as the blade torsional stiffness is not scaled down along with the reduced dynamic pressure, less blade twist will take place during these stability-derivative-measuring flights than during the actual pull-up maneuver. For a 10-percent reduction in forward and rotor speed, the dynamic pressure would be reduced approximately 20 percent from its usual value and hence approximately 20 percent of the blade twist occurring during the pull-ups would be missing. This error should be small except perhaps for blades of unusually low torsional stiffness or during conditions of extreme stall, when the chordwise position of the center of pressure is well behind the chordwise position of the center of gravity. Thus, equations (8) and (17) can be written with sufficient accuracy as follows:

$$\bar{L}_\alpha = \left(\frac{\Delta L}{\Delta \alpha}\right)_m \tag{34}$$

and

$$\bar{M}_\alpha = \left(\frac{\Delta M}{\Delta \alpha}\right)_m + \delta\left(M_\alpha\right)_r \tag{35}$$

where $\delta\left(M_\alpha\right)_r$ is given by equation (32).

For the special case of the single-rotor helicopter with no offset of the flapping hinges, equation (35) can be written

$$\bar{M}_{\alpha} = \left(\frac{\Delta M}{\Delta \alpha}\right)_m \frac{\Delta B_{1_c} + \delta \Delta B_{1_c}}{\Delta B_{1_c}} \tag{36}$$

where $\delta \Delta B_{1_c}$ is given by equation (33).

Damping-in-Pitch and Lift-Due-to-Pitching Derivatives

The measurement in flight of damping in pitch involves measuring the change in stick position, thrust coefficient, and rotor angle of attack in going from straight flight to steady turns at fixed values of pitch-lever position, throttle position, and forward speed. Preferably, $1\frac{1}{2}$- to 2-minute records should be taken at each condition. The rotor speed will probably increase somewhat in going to the turn condition, while the forward speed will vary some from the desired value. The change in stick position needed to neutralize pitching moments comes about from three causes, the angle-of-attack stability, the damping in pitch, and the change in tip-speed ratio. The contribution of angle-of-attack stability is computed with the use of the measured change in rotor angle of attack and the angle-of-attack stability measurements described in the previous section. If the lift due to pitching is small, as is normally the case, the measured change in thrust coefficient should be used in place of the measured change in rotor angle of attack because of greater probable experimental accuracy. The contribution of tip-speed-ratio change is obtained by measuring the change in tip-speed ratio and comparing with a plot of stick position against tip-speed ratio at constant pitch and throttle positions.

Correcting for the contributions of angle-of-attack stability and tip-speed-ratio change leaves the damping-in-pitch contribution to the change in stick position. Then, by use of equation (30) or (31), the pitching moment due to the pitching velocity can be computed. The pitching velocity itself can be measured, and the damping in pitch determined by dividing ΔM by q.

If any blade distortion takes place in going to the turn condition, it is caused by both the angle-of-attack changes and the pitching velocity. As discussed previously, the technique for measuring angle-of-attack stability accounts for only about 80 percent of the effects of dynamic blade

twist that occur during the pull-up maneuver. During the steady turns, however, the entire 100 percent is present. Thus, after the measured value of angle-of-attack stability has been subtracted, about 20 percent of the effect of blade twist due to angle-of-attack stability will remain in the measured damping in pitch. However, it might be pointed out that, by use of this technique for measuring damping in pitch, the effects of such errors in the measurement of angle-of-attack stability are minimized. If, for example, the measured angle-of-attack stability is in error on the side of too much instability, the damping in pitch will be in error on the side of too much damping in pitch. It can be seen from figure 2 that these two errors tend to compensate.

Thus, equation (16) can be written with sufficient accuracy as follows:

$$\bar{M}_q = \left(\frac{\Delta M}{q}\right)_m \tag{37}$$

In order to obtain the lift due to pitching, the contribution of the angle-of-attack change to the increase in C_T/σ in going to the turn condition is obtained from the lift-curve-slope measurements described previously and subtracted out, leaving the contribution of the pitching velocity to the change in C_T/σ.

Lift due to pitching velocity can be produced in the single-rotor helicopter if it is equipped with a gyroscopic device which changes longitudinal cyclic pitch in proportion to the pitching velocity. If the helicopter is so equipped, there is a resultant change in rotor angle of attack, and hence rotor thrust, with pitching velocity. Another possible source of lift due to pitching is a change in rotor stalling. A nose-up pitching velocity, for example, causes a forward tilt of the rotor tip-path plane with respect to the axis of no feathering. The accompanying upward blade flapping velocity on the retreating side reduces the blade-tip angle of attack. Thus, any retreating-tip blade stalling is reduced by a nose-up pitching velocity with a resultant increase in thrust at constant rotor angle of attack.

If no gyroscopic device is present and rotor stalling is not severe, the lift due to pitching is small and probably within the experimental accuracy in the measurement of the change in rotor angle of attack in going to the turn condition. If so, lift due to pitching is best assumed equal to zero.

It should be pointed out that it is desirable to make turns in both directions and average the results in order to eliminate such effects as pitching moments due to yawing velocity.

COMPUTATION OF STABILITY DERIVATIVES

Single-Rotor Helicopter

The pertinent longitudinal-stability derivatives for the single-rotor helicopter of figure 4 without and with a horizontal tail at approximately 70 knots indicated airspeed, level flight, are now computed by the techniques described in the previous section. The physical characteristics of this helicopter are listed in table I. These stability derivatives are used in part I for checking the chart presented herein.

Tail off.- Comparison between level-flight records at 70 knots indicated airspeed and records at reduced forward and rotor speed for the configuration without a horizontal tail indicates C_T/σ to increase by 0.020, the rotor angle of attack α to increase 4.2°, and the longitudinal cyclic pitch to change 0.43° in the forward direction (unstable). Thus

$$\frac{\Delta(C_T/\sigma)}{\Delta\alpha} = \frac{0.020}{4.2/57.3} = 0.27 \text{ per radian}$$

The trim value of C_T/σ is equal to 0.088. Thus, with the use of equation (34)

$$\frac{g\bar{I}_\alpha}{WV} = \frac{g}{WV}\frac{\frac{\Delta(C_T/\sigma)}{\Delta\alpha}}{(C_T/\sigma)_0}W$$

$$= \frac{32.2}{\frac{70}{\sqrt{0.9}}(1.467)(1.152)}\frac{0.27}{0.088}$$

$$= 0.8$$

Inasmuch as the single-rotor helicopter under study has no offset of the flapping hinges, equation (33) applies. Thus

$$\delta \Delta B_{1_c} = -\Delta B_{1_p} \frac{0.020/0.088}{1 + 0.020/0.088}$$

The value of ΔB_{1_p} measured during the pull-up maneuver to be used as a basis of comparison was -1.1°. Thus

$$\delta \Delta B_{1_c} = -(-1.1)0.185$$

$$= 0.20^\circ$$

Then using equations (30) and (36), with $\partial a'/\partial \alpha$ from reference 7, yields

$$\bar{M}_\alpha = \frac{0.43 + 0.20}{4.2}\left(1 + \frac{0.020}{0.088}\right)6.5(1 + 0.19)4900$$

$$= 7000 \text{ lb-ft/radian}$$

Thus

$$\frac{\bar{M}_\alpha}{I_Y} = \frac{7000}{7000}$$

$$= 1.0 \text{ lb-ft/radian/slug-ft}^2$$

The damping in pitch of the helicopter was measured at 65 knots, but the 5-knot difference in forward speed is not considered significant. The rotor stalling during the pull-up and the turn was not very severe. Thus, inasmuch as no gyroscopic device to change longitudinal cyclic pitch is present in the test helicopter, lift due to pitching is assumed equal to zero.

The following quantities were measured or computed for the test single-rotor helicopter in going from the level-flight condition to the steady-turn condition:

$$\Delta n = 0.26g$$

$$\Delta B_{1_c} = -0.61^\circ$$

$$\Delta\left(C_T/\sigma\right) = 0.019$$

$$\Delta\mu = 0$$

$$\Delta q = 0.12 \text{ radian/sec}$$

From angle-of-attack stability measurements at 65 knots, the effect of the angle-of-attack change on ΔB_1 was found to be 0.34°. This value was based on the change in C_T/σ in going into the turn, inasmuch as lift due to pitching is assumed equal to zero. Thus, correcting for $\Delta\mu$ and $\Delta\alpha$ yields

$$\Delta B_{1_c} = -0.61 - 0 - 0.34$$

$$= -0.95^\circ$$

$$= -0.016 \text{ radian}$$

Then substituting into equations (30) and (37), with $\partial a'/\partial\alpha$ obtained from reference 7, gives

$$\bar{M}_q = -\frac{0.016}{0.12}\left(1 + \frac{0.019}{0.088}\right)6.5(1 + 0.19)4900$$

$$= -6200 \text{ lb-ft/radian/sec}$$

Thus,

$$\frac{\bar{M}_q}{I_Y} = -\frac{6200}{7000} = -0.9$$

The modified angle-of-attack stability parameter for use in figure 3 is as follows:

$$\frac{\frac{\bar{M}_\alpha}{I_Y}\left(1 - \frac{g}{WV}\bar{L}_q\right) - \left(\frac{g}{WV}\bar{L}_q + E\right)E - \frac{\bar{M}_q}{I_Y}E + 0.70 + 0.58\left(\frac{\bar{M}_q}{I_Y} + E\right) + 0.12\left(\frac{\bar{M}_q}{I_Y} + E\right)^2}{\frac{g}{WV}\bar{L}_\alpha + E}$$

$$= \frac{1.0(1 - 0) - 0 - 0 + 0.70 + 0.58(-0.9) + 0.12(-0.9)^2}{0.8}$$

$$= 1.6$$

Tail on.- The single-rotor helicopter of figure 4 was equipped with the biplane tail surface shown in figure 6. The location and principal dimensions for the biplane tail surface are given in figure 7. The tail-surface incidence was 0° with respect to the rotor shaft.

The previously described procedures for measuring angle-of-attack stability, lift-curve slope, and damping in pitch were repeated for the tail-on condition.

The following values were obtained (with the lift due to pitching once again assumed to be equal to zero):

$$\frac{g}{WV}\bar{L}_\alpha = 0.8$$

$$\frac{\bar{M}_\alpha}{I_Y} = -0.3$$

$$\frac{\bar{M}_q}{I_Y} = -0.5$$

$$\frac{\frac{\bar{M}_\alpha}{I_Y}\left(1 - \frac{g}{WV}\bar{L}_q\right) - \left(\frac{g}{WV}\bar{L}_\alpha + E\right)E - \frac{\bar{M}_q}{I_Y}E + 0.70 + 0.58\left(\frac{\bar{M}_q}{I_Y} + E\right) + 0.12\left(\frac{\bar{M}_q}{I_Y} + E\right)^2}{\frac{g}{WV}\bar{L}_\alpha + E}$$

$$= 0.2$$

Tandem-Rotor Helicopter

The stability derivatives for the tandem-rotor helicopter of figure 5 at approximately 70 knots indicated airspeed in level flight and with power reduced approximately 50 percent are now computed by the previously described techniques. The physical characteristics of the helicopter are listed in table II. The center of gravity was approximately 13 inches forward of the midpoint between the rotors. These derivatives are used in part I to check the chart presented herein.

Level flight.- Comparison between level-flight records at 70 knots and records at reduced rotor and forward speed indicates C_T/σ to increase by 0.019, the rotor angle of attack α to increase by 5.8°, and the longitudinal cyclic pitch to change 0.42° in the forward direction (unstable). Thus,

$$\frac{\Delta(C_T/\sigma)}{\Delta\alpha} = \frac{0.019}{5.8/57.3} = 0.19 \text{ per radian}$$

Using equation (34) gives

$$\frac{g}{WV}\bar{L}_\alpha = \frac{g}{WV}\left(\frac{\Delta L}{\Delta\alpha}\right)_m = \frac{g}{WV}\frac{\frac{\Delta(C_T/\sigma)}{\Delta\alpha}}{(C_T/\sigma)_0}W$$

$$= \frac{32.2}{\frac{70}{\sqrt{0.9}}(1.467)(1.152)}\frac{0.19}{0.081} = 0.6$$

A change in stick position corresponding to -0.6° change in cyclic pitch was used during the pull-up maneuver to be used for comparison with the chart presented herein. Thus, from equation (32), with $\partial a'/\partial\alpha$ from reference 7,

$$\delta\bar{M}_{\alpha} = \frac{-(-0.6)}{57.3}(1 + 0.12)6\,\frac{0.19}{0.081}\,6700$$

$$= 1100 \text{ lb-ft/radian}$$

From equations (31) and (35), with $\partial a'/\partial\alpha$ and $\frac{\partial C_T/\sigma}{\partial\theta}$ from reference 7,

$$\bar{M}_{\alpha} = 2\,\frac{0.42}{5.8}\left(1 + \frac{0.019}{0.081}\right)6(1 + 0.12)\,\frac{6700}{2} +$$

$$\frac{0.42}{5.8}(1.0)(0.82)\,\frac{6700}{2(0.081)}\,\frac{42.3}{2} + 1100$$

$$= 57000 \text{ lb-ft/radian}$$

Thus,

$$\frac{M_{\alpha}}{I_Y} = \frac{57000}{40000} = 1.4$$

The damping in pitch of the tandem helicopter was measured by the turning technique described previously. Once again, the lift due to pitching is assumed equal to zero. After corrections were made for the contributions of angle-of-attack stability and tip-speed-ratio change, the change in longitudinal cyclic pitch was computed to be

$$-0.13 \text{ radian}/\text{radian/sec}$$

and the change in normal acceleration during the turn was 0.13g. Thus, using equations (31) and (37), again with $\partial a'/\partial\alpha$ and $\frac{\partial(c_T/\sigma)}{\partial\theta}$ from reference 7, yields

$$\bar{M}_q = -0.13(1 + 0.13)6(1 + 0.12)6700 +$$

$$(-0.13)(1.0)(0.82)\frac{6700}{2(0.081)}\frac{42.3}{2}$$

$$= -100000$$

Thus,

$$\frac{\bar{M}_q}{I_Y} = \frac{-100000}{40000} = -2.5$$

The modified angle-of-attack stability parameter for use in figure 3 is computed to be

$$\frac{\frac{\bar{M}_\alpha}{I_Y}\left(1 - \frac{g}{WV}\bar{L}_q\right) - \left(\frac{g}{WV}\bar{I}_\alpha + E\right)E - \frac{\bar{M}_q}{I_Y}E + 0.70 + 0.58\left(\frac{\bar{M}_q}{I_Y} + E\right) + 0.12\left(\frac{\bar{M}_q}{I_Y} + E\right)^2}{\frac{g}{WV}\bar{I}_\alpha + E}$$

$$= \frac{1.4(1 - 0) - 0 - 0 + 0.70 + 0.58(-2.5) + 0.12(-2.5)^2}{0.6}$$

$$= 2.3$$

Reduced power.- Repeating the previous procedure for the tandem helicopter at 70 knots indicated airspeed, power approximately one-half that for level flight, gives

$$\frac{g}{WV}\bar{L}_{\alpha} = 1.0$$

$$\frac{\bar{M}_{\alpha}}{I_Y} = -0.4$$

$$\frac{\bar{M}_q}{I_Y} = -1.7$$

$$\frac{\frac{\bar{M}_{\alpha}}{I_Y}\left(1 - \frac{g}{WV}\bar{L}_q\right) - \left(\frac{g}{WV}\bar{L}_{\alpha} + E\right)E - \frac{\bar{M}_q}{I_Y}E + 0.70 + 0.58\left(\frac{\bar{M}_q}{I_Y} + E\right) + 0.12\left(\frac{\bar{M}_q}{I_Y} + E\right)^2}{\frac{g}{WV}\bar{L}_{\alpha} + E}$$

$$= -0.3$$

CONCLUDING REMARKS

Because of the importance of maneuver stability for helicopter contact and instrument flying, a theoretical analysis of maneuver stability is made. The results are presented in the form of a chart which contains a boundary line separating satisfactory combinations of significant longitudinal stability derivatives from unsatisfactory combinations according to the criterion of normal-acceleration time history presented in NACA Technical Note 1983.

Good correlation is indicated for both a single-rotor helicopter and a tandem-rotor helicopter between maneuver stability as predicted by the chart and as measured during pull-up maneuvers. Thus, the theoretical analysis is indicated to be valid.

Techniques are described for measuring stability derivatives in flight. These derivatives are for use with the chart presented herein to aid in design studies of means for achieving satisfactory maneuver stability for a prototype helicopter or for a helicopter in the design stage that is similar to helicopters already flying.

In predicting maneuver stability of a new type of helicopter, the stability derivatives for use with the chart herein must be theoretically predicted. The problem remains of predicting these derivatives to the desired accuracy where significant amounts of rotor stalling are present.

Langley Aeronautical Laboratory,
National Advisory Committee for Aeronautics,
Langley Field, Va., June 9, 1953.

APPENDIX

EFFECT OF VARYING ROTOR SPEED

As indicated in the assumptions, a sample investigation of the effect of varying rotor speed during the pull-up maneuver was made. Additional terms accounting for the effect of changes in rotor speed on lift and pitching moment were added to equations (7) and (15), respectively. An equation for equilibrium of shaft torque was derived with rotor speed as the dependent variable. This equation contained terms accounting for the change in rotor torque and engine torque with rotor speed, the change in rotor torque with rotor angle of attack and pitching velocity, and the inertia torque. These three equations plus equation (19) were solved simultaneously by means of the Laplace transformation for a combination of parameters taken from figure 2. The computed time history of Δn became concave downward by 2.05 seconds. Thus the inclusion of rotor speed as an additional variable changed the time for the normal-acceleration time history to become concave downward by about 0.05 second, an insignificant amount.

The result presented in the previous paragraph is not too surprising in view of the compensating effects of rotor-speed variation. Permitting the rotor to speed up during the pull-up maneuver has two stabilizing effects, one due to the reduction in μ with a resulting nose-down moment due to the stability with μ of the rotor, the other due to the increased rotor lift-curve slope. These stabilizing effects are compensated by a destabilizing effect due to the rotor inertia. Because of the inertia of the rotor, changes in its speed lag behind changes in angle of attack. Thus, when the angle-of-attack time history becomes concave downward, the rotor-speed time history is still concave upward, so that the start of the downward concavity in the time history of lift and hence of normal acceleration is delayed.

REFERENCES

1. Gustafson, F. B.: Desirable Longitudinal Flying Qualities for Helicopters and Means to Achieve Them. Aero. Eng. Rev., vol. 10, no. 6, June 1951, pp. 27-33.

2. Crim, Almer, D., Reeder, John Paul, and Whitten, James B.: Initial Results of Instrument-Flying Trials Conducted in a Single-Rotor Helicopter. NACA TN 2721, 1952.

3. Gustafson, F. B., Amer, Kenneth B., Haig, C. R., and Reeder, J. P.: Longitudinal Flying Qualities of Several Single-Rotor Helicopters in Forward Flight. NACA TN 1983, 1949.

4. Myers, Garry C., Jr.: Flight Measurements of Helicopter Blade Motion With a Comparison Between Theoretical and Experimental Results. NACA TN 1266, 1947.

5. Gessow, Alfred, and Amer, Kenneth B.: An Introduction to the Physical Aspects of Helicopter Stability. NACA Rep. 993, 1950. (Supersedes NACA TN 1982.)

6. Churchill, Ruel V.: Modern Operational Mathematics in Engineering. McGraw-Hill Book Co., Inc., 1944.

7. Amer, Kenneth B., and Gustafson, F. B.: Charts for Estimation of Longitudinal-Stability Derivatives for a Helicopter Rotor in Forward Flight. NACA TN 2309, 1951.

8. Amer, Kenneth B.: Theory of Helicopter Damping in Pitch or Roll and a Comparison With Flight Measurements. NACA TN 2136, 1950.

9. Bailey, F. J., Jr.: A Simplified Theoretical Method of Determining the Characteristics of a Lifting Rotor in Forward Flight. NACA Rep. 716, 1941.

10. Bailey, F. J., Jr., and Gustafson, F. B.: Charts for Estimation of the Characteristics of a Helicopter Rotor in Forward Flight. I - Profile Drag-Lift Ratio for Untwisted Rectangular Blades. NACA WR L-110, 1944. (Formerly NACA ACR L4H07.)

11. Gustafson, F. B.: Flight Tests of the Sikorsky HNS-1 (Army YR-4B) Helicopter. I - Experimental Data on Level-Flight Performance With Original Rotor Blades. NACA WR L-595, 1945. (Formerly NACA MR L5C10.)

TABLE I.- APPROXIMATE PHYSICAL CHARACTERISTICS OF

SINGLE-ROTOR HELICOPTER

Gross weight, lb	4,900
Pitching moment of inertia about center of gravity, slug-ft^2	7,000
Height of rotor hub with respect to center of gravity, ft	6.5
Offset of flapping hinge from center line of rotor shaft, ft	0
Number of blades	3
Rotor diameter, ft	48
Tip-speed ratio, μ	0.25
Solidity (chord weighted according to radius^2), σ	0.063
Density ratio	0.9
Ratio of thrust coefficient to solidity, C_T/σ	0.088
Blade mass factor (ratio of air forces to inertia forces)	9
Longitudinal cyclic pitch per inch of stick deflection, deg	0.8

TABLE II.- APPROXIMATE PHYSICAL CHARACTERISTICS

OF TANDEM HELICOPTER

Gross weight, lb	6,700
Pitching moment of inertia, slug-ft^2	40,000
Height of rotor hub with respect to center of gravity, ft	6
Assumed offset of flapping hinge from center line of rotor shaft	0
Number of rotors	2
Number of blades per rotor	3
Diameter of each rotor, ft	41
Distance between rotor shafts, ft	42.3
Tip-speed ratio, μ	0.23
Solidity (chord weighted according to radius^2), σ	0.052
Density ratio	0.9
Ratio of thrust coefficient to solidity, C_T/σ	0.081
$\frac{\partial \Delta\theta}{\partial B_1}$	1.0
Longitudinal cyclic pitch per inch of stick deflection, deg	1.0
Blade mass factor (ratio of air forces to inertia forces)	9
Horizontal stabilizer area, sq ft	40
Total vertical stabilizer area, sq ft	50
Allowable center-of-gravity range, in. forward of midpoint between rotors	-1 to 18

NACA

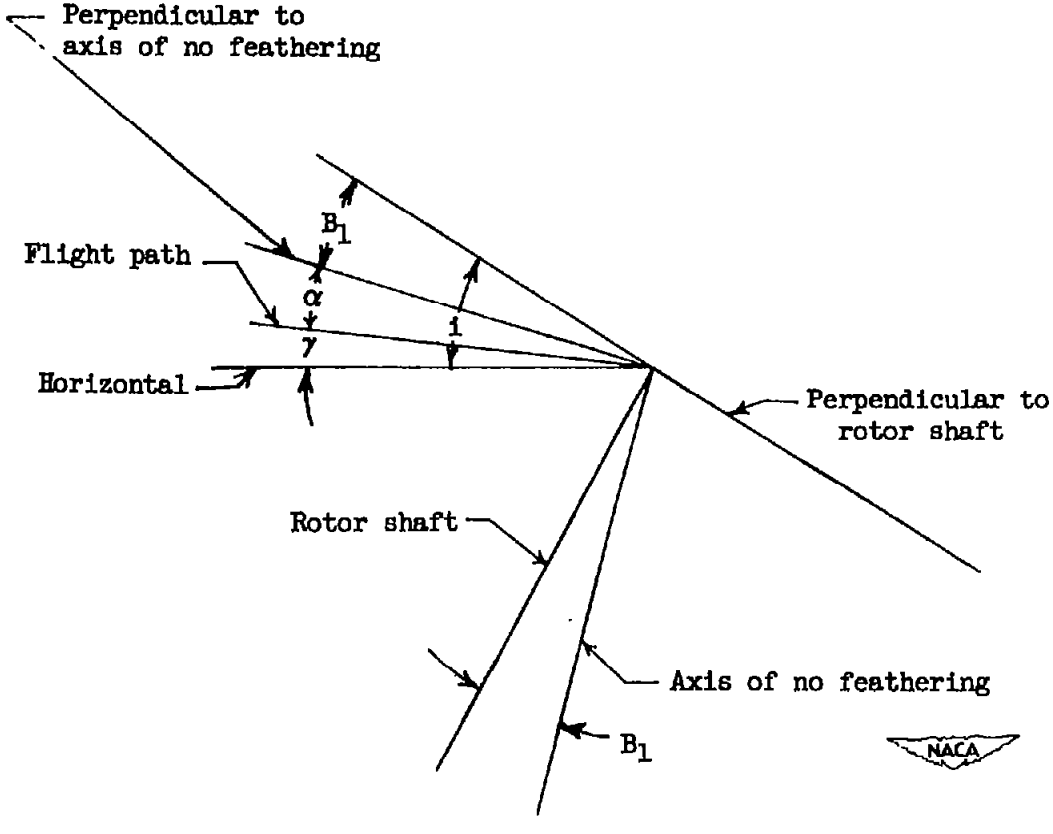

Figure 1.- Relation between rotor angle of attack, rotor-shaft incidence, angle of climb, and longitudinal cyclic pitch. All angles shown are positive. Axis of no feathering is uncorrected for blade and control-system distortion, δ_3, or automatic control devices.

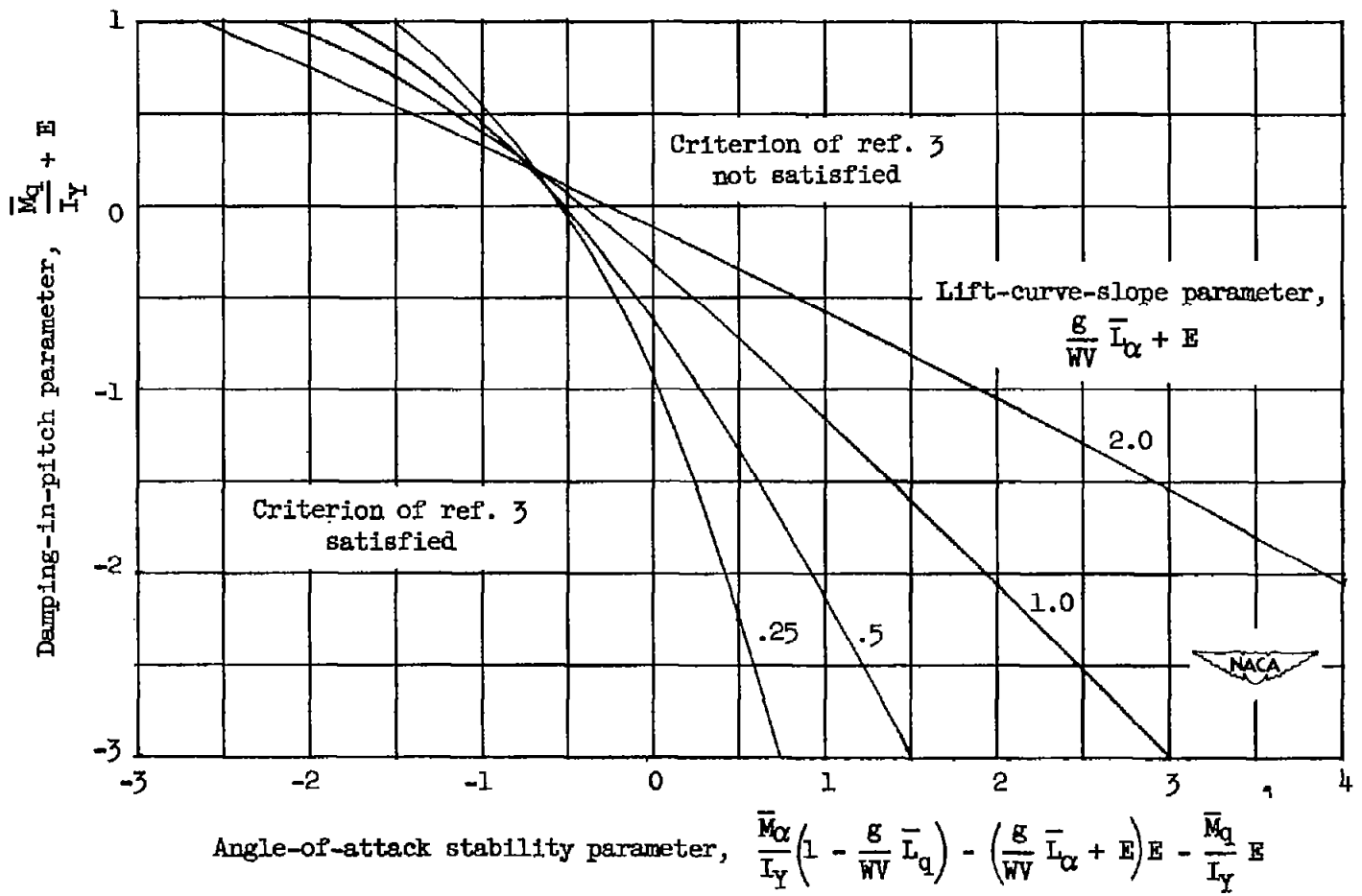

Figure 2.- Damping-in-pitch parameter plotted against angle-of-attack stability parameter for various values of lift-curve-slope parameter for marginal maneuver stability. $E \approx \frac{\bar{L}_{\dot{\alpha}}}{\bar{L}_\alpha}\frac{\bar{M}_{B_1}}{I_Y}$.

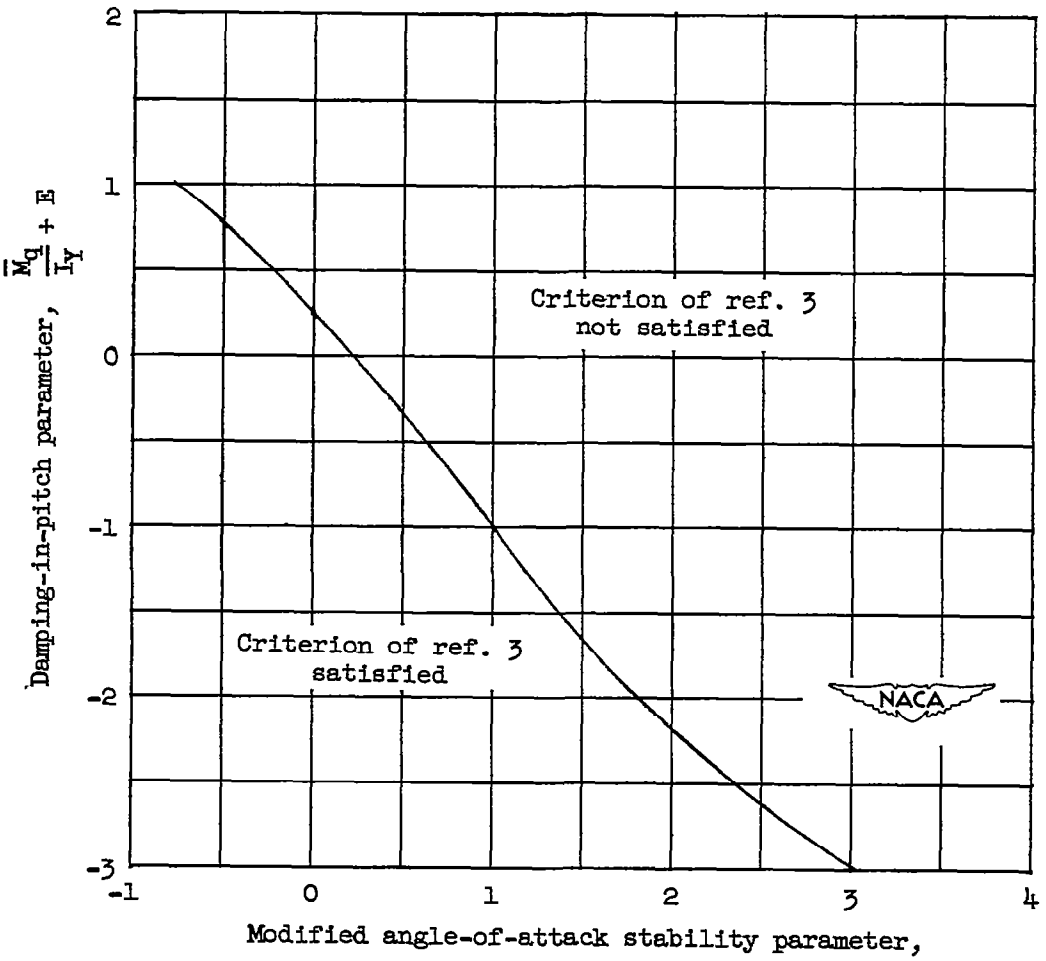

Figure 3.- Damping-in-pitch parameter plotted against modified angle-of-attack stability parameter for marginal maneuver stability.

$$E \approx \frac{\bar{L}_q}{\bar{L}_\alpha}\frac{M_{\bar{B}_1}}{I_Y}.$$

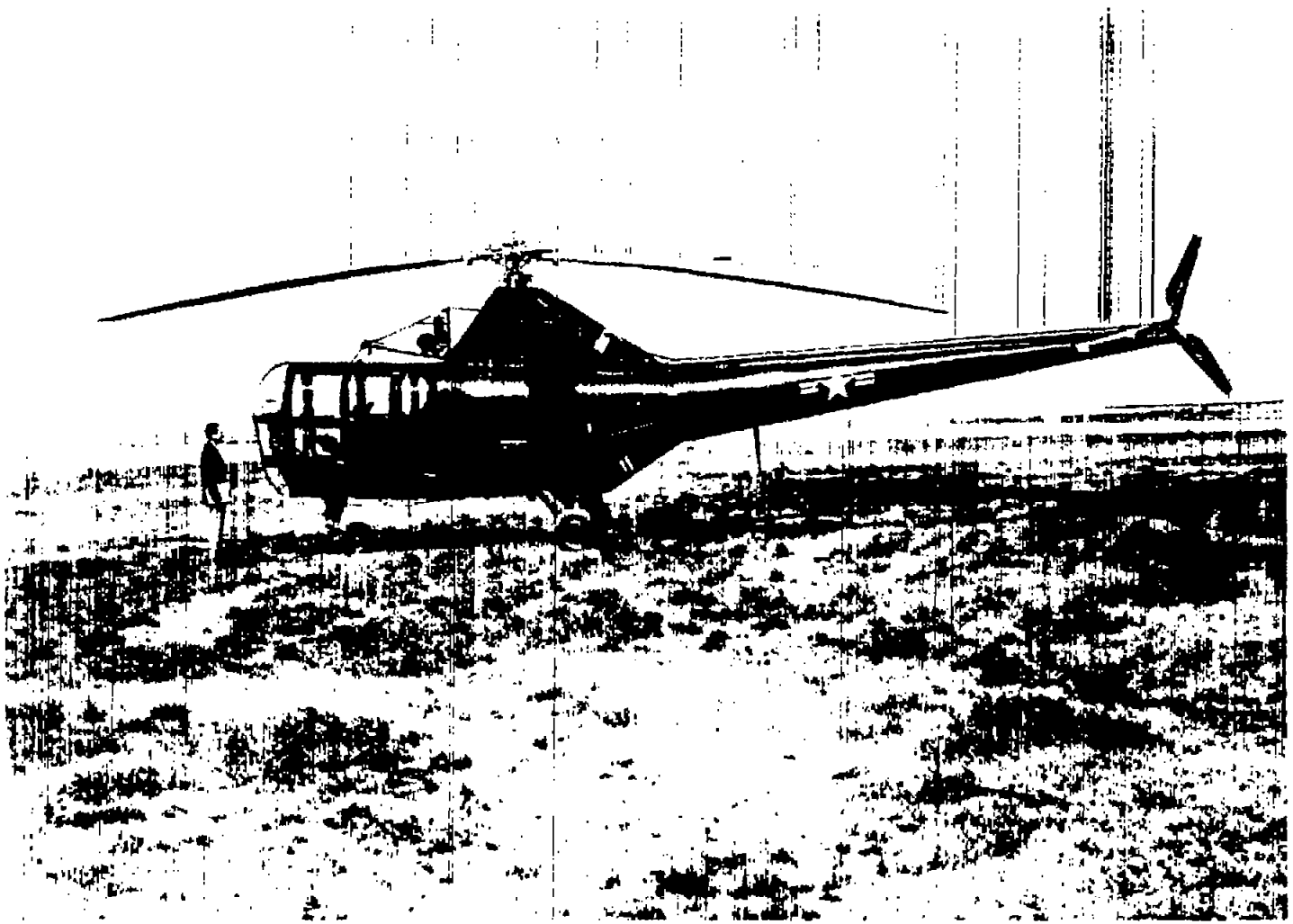

Figure 4.- Single-rotor helicopter studied in this paper. L-55866.1

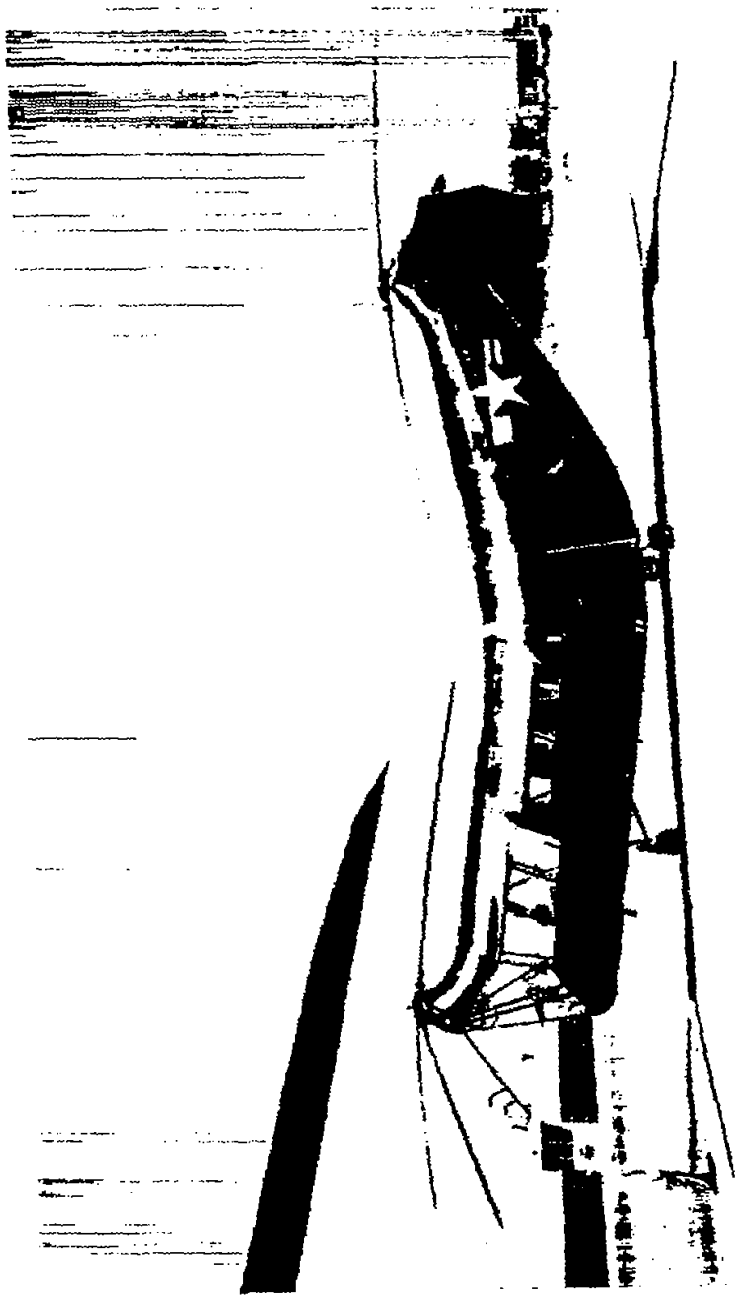

Figure 5.- Tandem-rotor helicopter studied in this paper.

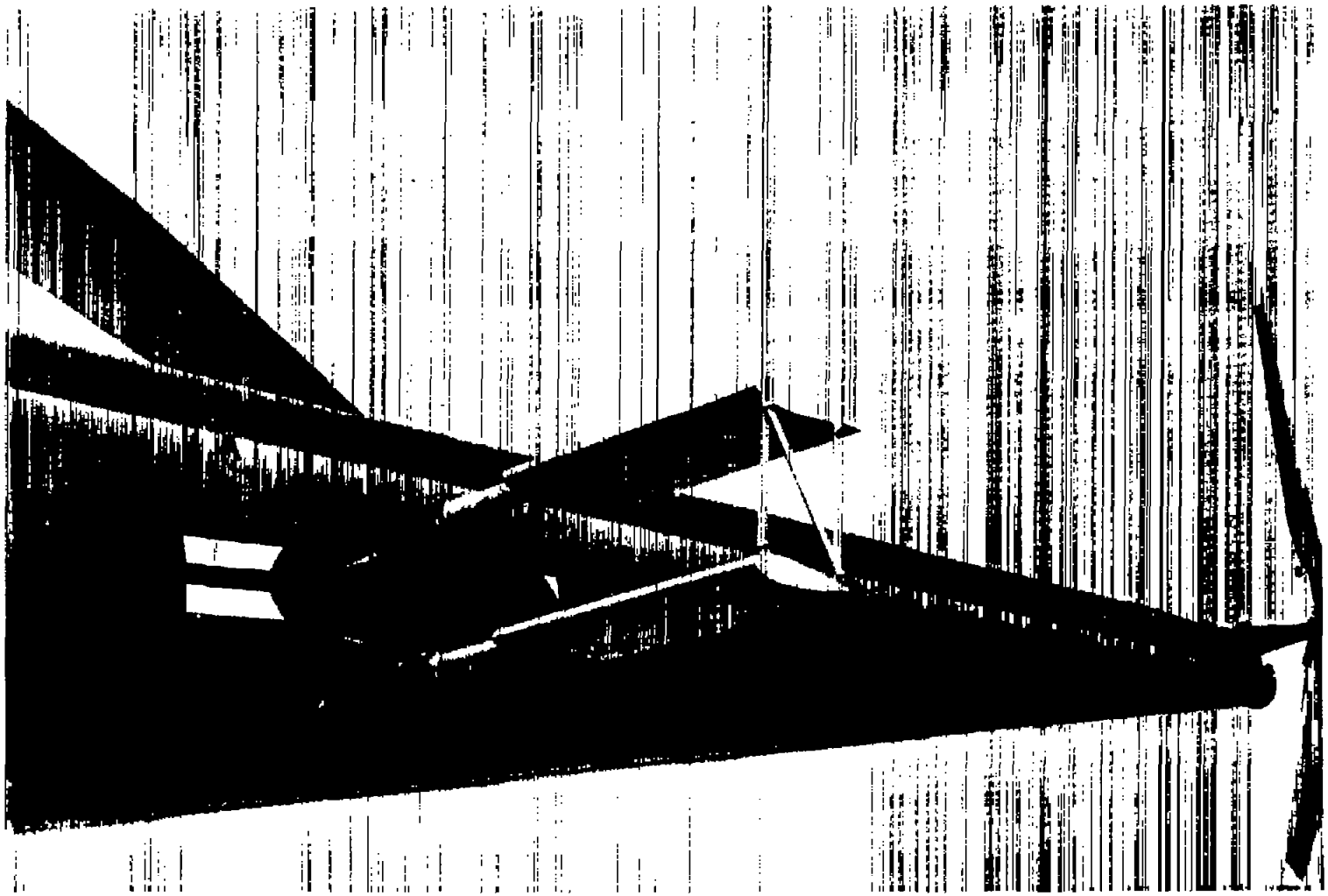

Figure 6.- Biplane tail surface used to vary angle-of-attack stability of single-rotor helicopter.

L-58392.1

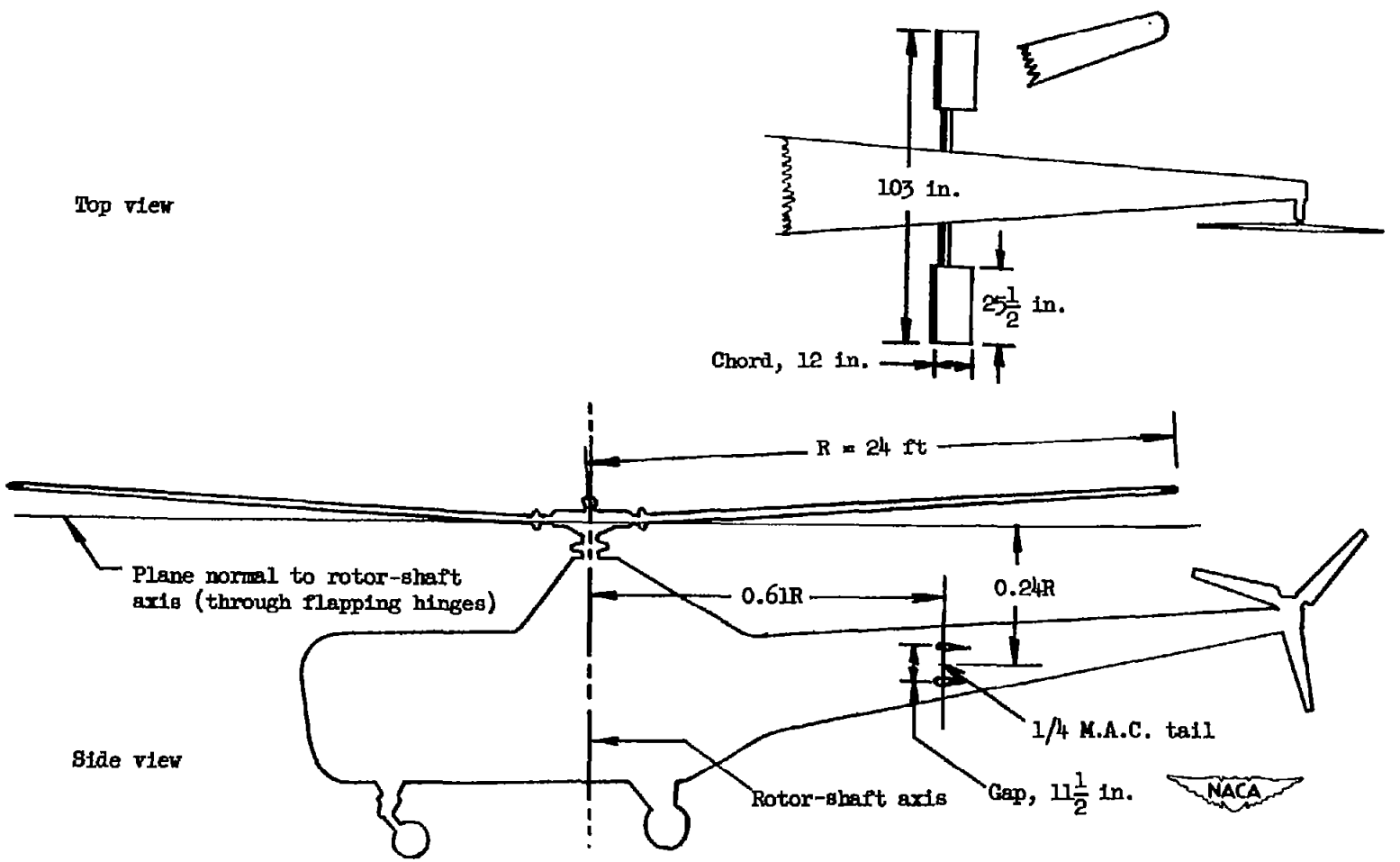

Figure 7.- Location and principal dimensions of biplane tail surface used to vary angle-of-attack stability of single-rotor helicopter. Angle of incidence of tail surface is 0° or 7° relative to plane normal to rotor-shaft axis.

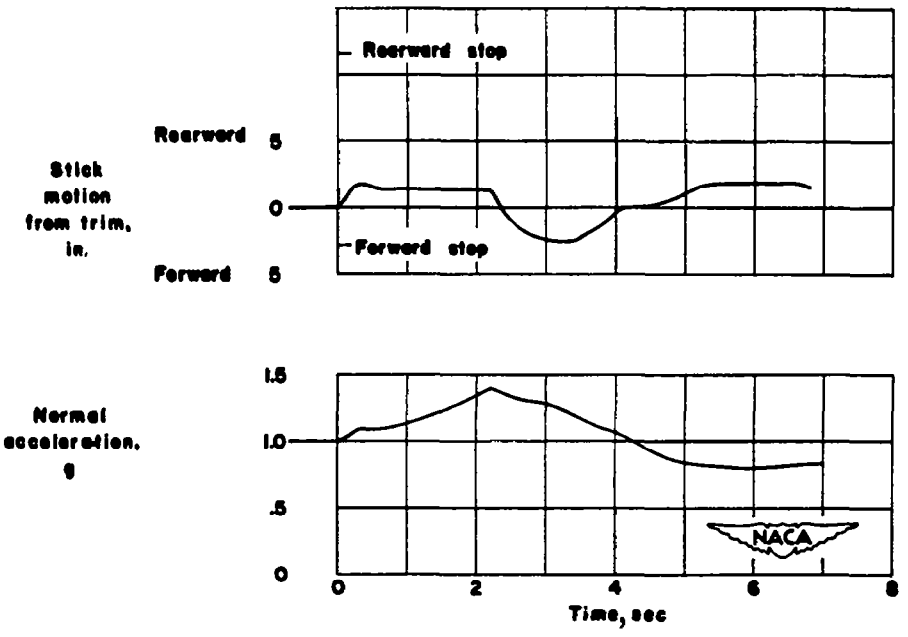

(a) Single-rotor helicopter, level flight, tail off.

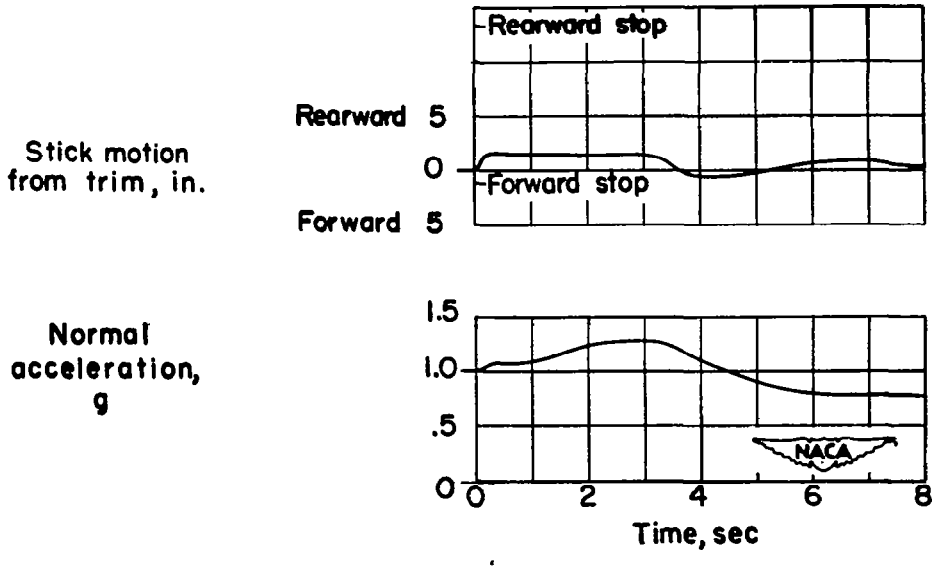

(b) Single-rotor helicopter, level flight, tail on at 0°.

Figure 8.- Time histories of pull-up maneuvers for test helicopters at approximately 70 knots.

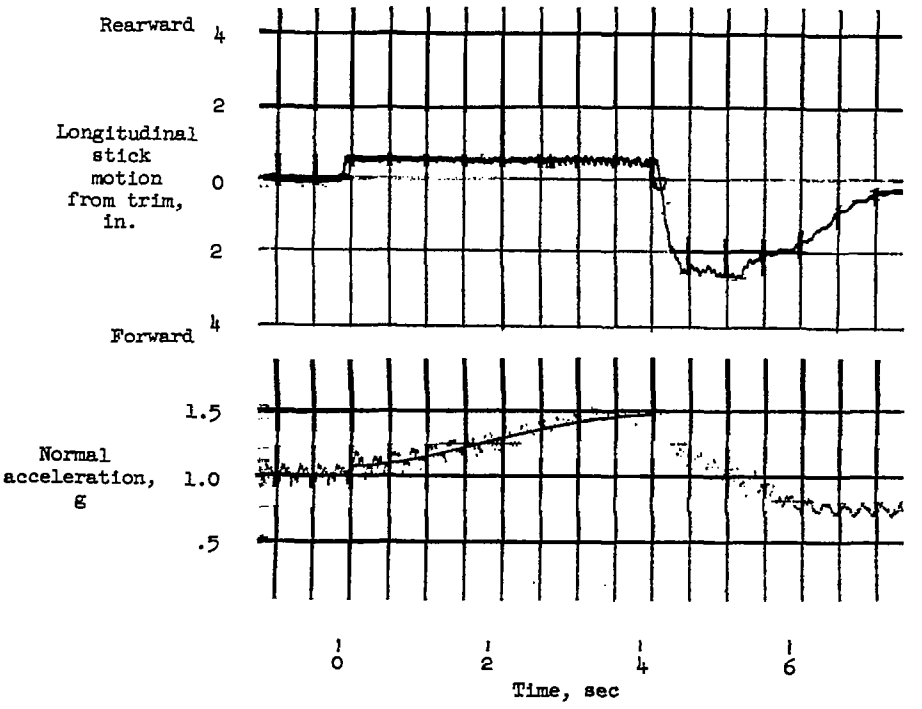

(c) Tandem-rotor helicopter, forward center of gravity, level flight.

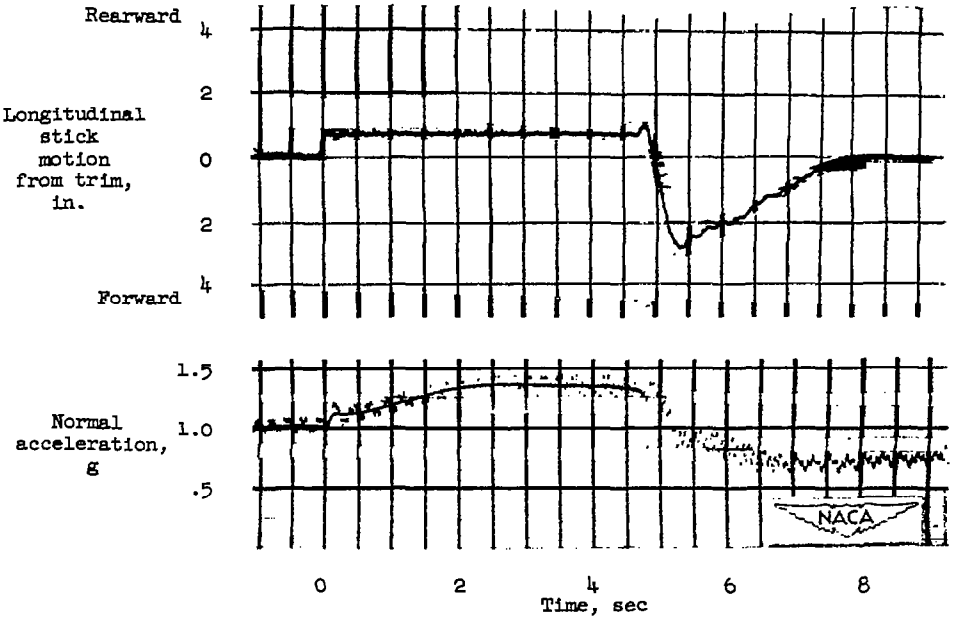

(d) Tandem-rotor helicopter, forward center of gravity, partial-power descent.

Figure 8.- Concluded.

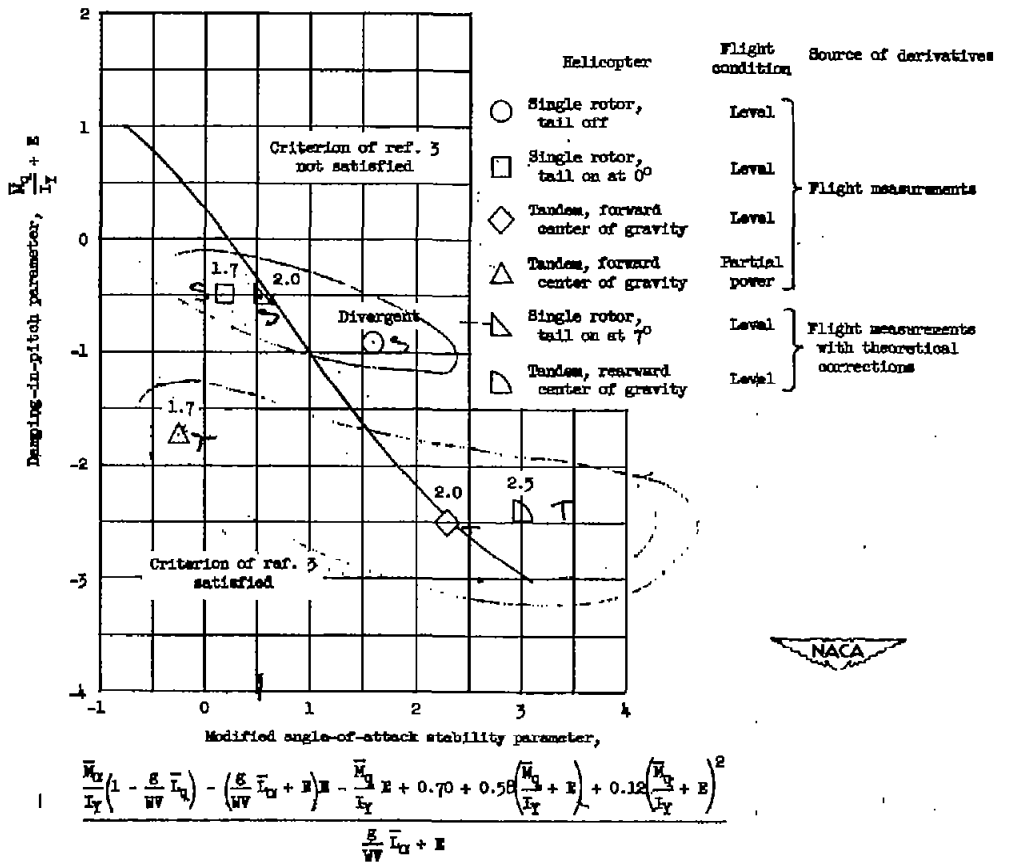

Figure 9.- Comparison of maneuver stability predicted from measured stability derivatives and from pull-up time histories such as in figure 8. The times for the normal-acceleration time history during the pull-up to become concave downward are noted above the data points. $E \approx \frac{\bar{L}_q}{\bar{L}_\alpha}\frac{M_{B_1}}{I_Y}$.

NACA-Langley - 10-28-53 - 1000